

AD-A267 956



MENTATION PAGE

Form Approved

OMB No. 0704-0188

Estimated to average 1 hour per response, including the time for reviewing instructions, searching existing data sources, gathering and reviewing the collection of information, sending comments regarding this burden estimate or any other aspect of this burden, to Washington Headquarters Services, Directorate for Information Operations and Reports, 1215 Jefferson to the Office of Management and Budget, Paperwork Reduction Project (0704-0188), Washington, DC 20503.

1. AGENCY USE ONLY (Leave blank)		2. REPORT DATE June 1993		3. REPORT TYPE AND DATES COVERED THESIS/DISSERTATION	
4. TITLE AND SUBTITLE OPTIMIZATION OF SATELLITE COVERAGE IN OBSERVING CAUSE AND EFFECT CHANGES IN THE IONOSPHERE, MAGNETOSPHERE, AND SOLAR WIND				5. FUNDING NUMBERS	
6. AUTHOR(S) Capt Martin Jay Loveliss					
7. PERFORMING ORGANIZATION NAME(S) AND ADDRESS(ES) AFIT Student Attending: Utah State University				8. PERFORMING ORGANIZATION REPORT NUMBER AFIT/CI/CIA- 93-118	
9. SPONSORING / MONITORING AGENCY NAME(S) AND ADDRESS(ES) DEPARTMENT OF THE AIR FORCE AFIT/CI 2950 P STREET WRIGHT-PATTERSON AFB OH 45433-7765				10. SPONSORING / MONITORING AGENCY REPORT NUMBER	
11. SUPPLEMENTARY NOTES					
12a. DISTRIBUTION / AVAILABILITY STATEMENT Approved for Public Release IAW 190-1 Distribution Unlimited MICHAEL M. BRICKER, SMSgt, USAF Chief Administration				12b. DISTRIBUTION CODE	
13. ABSTRACT (Maximum 200 words) <div style="text-align: center;"> </div> <div style="text-align: right;"> 93-19023 </div>					
14. SUBJECT TERMS				15. NUMBER OF PAGES 93	
				16. PRICE CODE	
17. SECURITY CLASSIFICATION OF REPORT		18. SECURITY CLASSIFICATION OF THIS PAGE		19. SECURITY CLASSIFICATION OF ABSTRACT	
				20. LIMITATION OF ABSTRACT	

OPTIMIZATION OF SATELLITE COVERAGE IN OBSERVING
CAUSE AND EFFECT CHANGES IN THE IONOSPHERE,
MAGNETOSPHERE, AND SOLAR WIND

by

Martin Jay Loveless

A thesis submitted in partial fulfillment
of the requirements for the degree

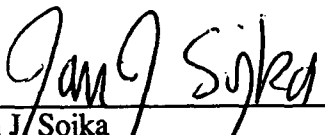
of

MASTER OF SCIENCE

in

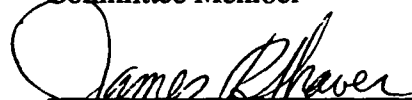
Physics

Approved:


Jan J. Sojka
Major Professor


W. Farrell Edwards
Committee Member


Kent L. Miller
Committee Member


James P. Shaver
Dean of Graduate Studies

UTAH STATE UNIVERSITY
Logan, Utah

1993

ACKNOWLEDGMENTS

I would like to acknowledge the guidance and patience of Dr. Jan J. Sojka, my advisor, and my other committee members, Drs. Kent Miller and Farrell Edwards, whose cooperation was greatly appreciated while doing this research. The plots that appear in this thesis are a result of the plotl program courtesy of Don Thompson. I would also like to thank William B. (Trey) Cade, Ricardo C. Davila, and Teresa Burns for their subjective additional analysis of the curves used in this study. I would like to thank Shawna Johnson and Melanie Oldroyd for their help with computer questions and other problems that arose. I would like to thank all my fellow Air Force students stationed here at USU who offered support throughout. Finally, I'd like to thank all my friends and family for all their support during my studies here at Utah State University.

Martin Jay Loveless

DTIC QUALITY INSPECTION

Accession For	
NTIS GRA&I	<input checked="checked" type="checkbox"/>
DTIC TAB	<input type="checkbox"/>
Unannounced	<input type="checkbox"/>
Justification	
By	
Distribution/	
Availability Codes	
Dist.	Avail and/or Special
A-1	

CONTENTS

	Page
ACKNOWLEDGMENTS.....	ii
LIST OF TABLES.....	v
LIST OF FIGURES.....	vii
ABSTRACT.....	ix
CHAPTER	
1. INTRODUCTION.....	1
2. ENERGY TRANSFER FROM SUN TO IONOSPHERE.....	6
2.1 SOLAR WIND-MAGNETOSPHERIC COUPLING.....	6
2.2 MAGNETOSPHERIC-IONOSPHERIC COUPLING.....	7
2.3 FIELD-ALIGNED CURRENTS.....	9
2.4 IONOSPHERIC-THERMOSPHERIC COUPLING.....	12
3. IONOSPHERIC OBSERVATIONS AND MODEL COMPARISON PROCEDURES.....	14
3.1 METHOD OF OBSERVATION.....	14
3.2 LIMITATIONS OF DATA.....	15
3.3 INTERNATIONAL REFERENCE IONOSPHERE.....	19
3.4 TIME DEPENDENT IONOSPHERIC MODEL.....	21
3.5 DATA VERSUS MODEL COMPARISONS.....	22
4. OBSERVATIONS VERSUS MODEL COMPARISONS.....	26
4.1 CHOOSING ORBITS FOR ANALYSIS.....	26
4.2 EXAMPLE OF CURVE COMPARISONS.....	28
4.3 STATISTICAL COMPARISON.....	29
4.4 QUALITATIVE COMPARISONS.....	34
4.5 OTHER INTERPRETATIONS OF THE CURVES.....	38
5. ANALYSIS OF DATA.....	43
5.1 TROUGH REGION.....	43
5.2 POLAR CAP REGION.....	51
5.3 AURORAL REGION.....	59
5.4 MID-LATITUDE REGION.....	65
5.5 SUMMARY.....	69
6. CONCLUSIONS.....	70

	iv
REFERENCES.....	85
APPENDIX.....	87

LIST OF TABLES

Table	Page
1 The listing of average monthly Kp's and sunspot numbers.....	19
2 TDIM climatology data base conditions.....	22
3 Data from northward IMF.....	24
4 Data from southward IMF.....	25
5 Breakout of observations by Kp values and seasons.....	28
6 Statistical average difference between observations and models.....	35
7 Standard deviation average difference between observations and models.....	36
8 Qualitative difference between observations and models.....	39
9 Qualitative difference between observations and models.....	40
10 Qualitative difference between observations and models.....	41
11 Qualitative difference between observations and models.....	42
12 Specifications of the trough region.....	48
13 Specifications of the polar cap region.....	60
14 Specifications of the auroral region.....	65
15 Specifications of the mid-latitude region.....	69
16 Advantages and disadvantages of ground-based stations alone.....	75
17 Parameters that should be measured on a smaller time scale.....	78
18 Advantages and disadvantages of satellites (one orbit only).....	80
19 One orbit plane configuration (Scenario 1).....	80
20 Advantages and disadvantages of 2 or more different orbits.....	81
21 Two orbit plane configuration (Scenario 2).....	83
22 Advantages and disadvantages of both ground-based stations and satellites.....	83
23 Northward IMF breakdown into regions.....	88

		vi
24	Southward IMF breakdown into regions.....	89
25	Curve comparisons for trough conditions.....	90
26	Curve comparisons for mid-latitude conditions.....	91
27	Curve comparisons for auroral oval conditions.....	92
28	Curve comparisons for polar cap conditions.....	93

LIST OF FIGURES

Figure		Page
1	Process by which energy from solar wind interacts with the magnetosphere and eventually exits the magnetosphere and heads for the ionosphere.....	8
2	Exactly the same as Figure 1 except that this figure represents disturbed time conditions.....	8
3	Sample data from the DE-2 microfiche showing data for September 20, 1982, orbit number 6215.....	16
4	Same as Figure 3 except data is for August 27, 1981, orbit number 351.....	17
5	A plot of the orbits of DE-2 satellite.....	20
6	This figure shows an example of agreement between the TDIM curve (plus sign symbol) and the observations (octagon shaped symbol).....	30
7	This figure shows an example of good agreement between the IRI and the observations.....	31
8	An example of a case where neither IRI nor TDIM model agrees with the observed curve at all.....	32
9	Another example of no agreement between the models and the observations.....	33
10	Clarification of definitions of terms.....	37
11	This figure shows the plasma convection paths as well as the position of the auroral oval. The mid-latitude trough lies equatorward of this auroral region boundary.....	45
12	This figure shows relatively good agreement between the TDIM and the DE-2 observations.....	47
13	This is a figure where the model and the observations are not in very good agreement.....	49
14	An example of a tongue of ionization from the DE-2 data.....	53
15	The TDIM model plot showing the tongue of ionization.....	54
16	An example of a polar hole in the DE-2 data.....	57
17	The TDIM plot for the same time frame as Figure 16.....	58
18	This figure shows good agreement between the observations and the model.....	63

19	An example of poor agreement between the observations and the model.....	64
20	An example of good agreement between the model and the observation.....	67
21	An example of poor agreement between the curves for the mid-latitude region.....	68
22	This figure shows approximate spacing required for satellite constellation to give a 10-minute interval between points.....	77
23	One of many possibilities for coverage of the ionosphere using more than one orbit (2 in this case).....	82

ABSTRACT

Optimization of Satellite Coverage in Observing Cause and Effect Changes in the Ionosphere, Magnetosphere, and Solar Wind

by

Martin J. Loveless, Master of Science

Utah State University, 1993

Major Professor: Dr. Jan J. Sojka
Department: Physics

Disturbances in the ionosphere sometimes cause adverse effects to communications systems, power grids, etc. on the earth. Currently, very little, if any, lead time is given to warn of an impending problem. If a forecast could be made of ionospheric occurrences, some lead time may be given to appropriate agencies and equipment may be saved. Most changes that occur in the ionosphere are a result of interaction of energy, currents, etc. between the magnetosphere and/or solar wind. Before a forecast can be made, however, improvement of ionospheric models currently in use need to be made. The models currently depict features in various regions of the ionosphere but not always where these features are actually observed. So an improvement to the model is needed to create an accurate baseline condition, or in other words an accurate depiction of the current ionosphere. Models could be improved by inputting real-time data from the ionosphere into the model. This data would come from satellites and/or ground-based stations.

It was found from my research that ionospheric regions rarely have boundaries with the exception of some mid-latitude troughs. The trough and polar cap regions both have features which can be "tracked" (followed) over time. Diurnal variation and seasonal effects in the F region along with this tracking of the regions are more than one satellite can

measure. A constellation of satellites in more than one orbit is required to give total and constant coverage of the entire ionosphere. These satellite observations can be complemented by observations from the ground stations, but ground station data alone would not be adequate for total ionospheric coverage. A combination of satellites and ground-based stations would give enough information that could be input to the models to establish a baseline condition. Once this baseline is established, an attempt at forecasting can be made.

(103 pages)

CHAPTER 1

INTRODUCTION

The radiation from the sun contains sufficient energy at short wavelengths to cause appreciable photoionization of the Earth's atmosphere at high altitudes, resulting in a partially ionized region known as the ionosphere [Tascione, 1988]. Some of this solar energy first interacts with the magnetosphere where this solar energy acts as a driver of processes in the magnetosphere, and some of the energy from the magnetosphere eventually interacts with the ionosphere. The thermosphere also provides energy input to the ionosphere but at a more delayed rate than the magnetosphere. It is this change in energy (increase or decrease) that is a cause of the change of conditions in the ionosphere. Many of these changes in the ionosphere can be observed as they are happening or the effects may be able to be seen after a change has taken place. Unfortunately, the ability to forecast when or where these changes will take place or the effects that result from the change in the ionosphere is very poor.

A drastic change in the status of the ionosphere can cause severe damage or disruption to certain communication systems used by the United States military as well as other private interests such as telephone companies, etc. Instrumentation aboard satellites used for transmission or relay of information for various organizations can be severely damaged or degraded. One effect of a geomagnetic storm, which is the cause of most of these ionospheric changes, is that it has caused power grids on the ground to literally blow up. So a loss of power or communication systems resulting from an ionospheric disturbance could be detrimental to any of us at any time. In fact, many of the organizations with interest in ionospheric disturbance effects met in Ottawa, Canada in May, 1992 to discuss these problems.

Physics plays an important part in ionospheric conditions. There are different regions in the ionosphere. Different features (troughs, auroras, etc.) are noted in each region so it

is not always possible to concentrate on just one feature or region. Interaction occurs between these ionospheric regions, i.e., by neutral winds, gravity waves, turbulence, diffusion, etc., just to name a few. Interaction (coupling) also occurs not only within the ionosphere but also between other regions in the solar terrestrial environment. For example, changes that occur in the magnetosphere may affect changes in the ionosphere, i.e., energy input from the magnetosphere causes changes in the ionosphere of many factors (temperatures, densities, composition of particles, just to name a few). The ionosphere is also interacting (coupling) back with the magnetosphere as well as interacting (coupling) with the thermosphere. So, the regions of the ionosphere are interacting with each other and they also may be interacting with regions outside the ionosphere as well. Also, physical changes, such as seasons, geomagnetic conditions, solar radio flux (F10.7) and even time of day have separate and varying effects on the physical processes occurring in these ionospheric regions.

The research conducted here analyzed electron density in the ionosphere. It has been observed that although there are many kinds of changes in ionospheric parameters (energy input, currents, temperatures, etc.) most of them are directly correlated with electron density (increasing or decreasing). Energy from the magnetosphere, in the form of particle precipitation, acts to change the density in the auroral region, as an example. Therefore, if the electron density over an ionospheric region is monitored, it can be seen what ionospheric changes are taking place and perhaps a forecast could be made and interested agencies or organizations could be notified so that precautions might be taken, if needed, to avoid or reduce the damage to systems, equipment, etc. The forecast lead time would be dependent on the user requirements. However, the lead time of the forecast would probably be from minutes to tens of minutes. Monitoring the features (troughs, auroras, etc.) and the movement of the features by monitoring the density maximums or minimums could aid in forecasting ionospheric events.

Several models have been created to try to model the ionosphere. There are both empirical models (models which are based on observable data) and physical models (models which use math, etc.) which are used to model the regions. Weaknesses exist in these models. One weakness is that data is averaged in statistical models, which may cause the obvious occurrence of an anomaly to be damped or done away with totally. Another weakness is that inputs to dynamic physical models are statistical. Unfortunately, as with most models, some assumptions usually need to be made. These assumptions may include deleting factors that "aren't so important" or perhaps even factors which may occasionally be observed but cannot otherwise be explained. Inconsistencies may exist in the model output that could cause misinterpretation or misrepresentation of the data.

Currently, ground-based stations exist that monitor the ionosphere constantly but the location of these ground-based stations is limited by political and geographic factors and "global" coverage is not possible. Satellites, on the other hand, do not have these political and geographic restrictions so with the proper arrangement they can monitor the ionosphere better. Most of the emphasis of this thesis is on satellite usage.

Currently, there are a few geostationary satellites and a few orbiting satellites that are being used to observe ionospheric regions. However, in the case of geostationary satellites, the same place in the ionosphere is being looked at over and over, and for orbiting satellites, the pass made through the ionospheric region(s) of interest is for a brief time only. In both cases, there is plenty of time and space not being observed where significant changes or occurrences can be taking place. One purpose of this thesis is to look at the least number of satellites required and their arrangement (spacing) to give the maximum ionospheric coverage on a continuous basis to aid in forecasting ionospheric events.

A fairly extensive data base of observable electron density exists from the Dynamic Explorer 2 (DE-2) satellite. By running the International Reference Ionosphere (IRI)

model (an empirical model) and the Time Dependent Ionospheric Model (TDIM) (a physical model), the electron density output from these models are able to be compared with actual electron density observations. From these comparisons it may be obvious if the model detects or depicts certain parameters or features inconsistently or incorrectly by incorrectly depicting features such as troughs, auroras, etc. Perhaps if a pattern could be seen in the inconsistencies, then empirical model improvement could take place. This improvement, however, could cause an established or well represented parameter to change and thus give wrong information also. So caution needs to be exercised when "improving" models. It will be these types of models which will be used to forecast occurrences in the ionosphere, so the way the models depict the current ionosphere is important.

This thesis will start out with an overview of the regions and the various "drivers" in these regions. A strong emphasis will be made on electrodynamic coupling by regions, electrical current, and energy drivers. Also, the ionosphere will be divided into its regions with currents associated with these regions discussed. This will comprise Chapter 2.

In Chapter 3, ionospheric observations and model comparisons will be discussed. A description of models used as well as limitations of the models will be discussed. A discussion of the observed data will be made as well as a discussion of comparisons procedures between models and observations. Data will be discussed as to its availability, selection, and limitations.

Chapter 4 will include a quantitative and qualitative comparison of the models versus the observations. The first section of this chapter will address how the orbits were chosen for analysis. Following in the next section will be examples of curve comparisons. The third section will address the statistical aspects of the comparisons and the final section of this chapter will deal with qualitative comparisons.

Chapter 5 will follow with an analysis of the data and a discussion of the various regions of the ionosphere (polar cap, auroral, mid-latitude, and trough) and how the data

fits into each of those regions. The physics of each of these regions will be discussed as well as how the models handle the data relative to each region.

Finally, Chapter 6 will include conclusions from the analysis and various interpretations that have been done. This will include a discussion of the constellation (arrangement) of the minimum number of satellites needed to give adequate coverage of the ionosphere to establish a current depiction of the ionosphere in the models.

The initial goal of this research was to see if a forecast of ionospheric changes could be made. This involved using both physical and empirical models. It was discovered that forecasting in the present state is almost impossible since the models do not model the present day ionosphere very accurately. Until an accurate baseline is created in the models, forecasting will be almost impossible as is shown in this thesis. This baseline is possible by using continuously monitoring satellites.

CHAPTER 2

ENERGY TRANSFER FROM SUN TO IONOSPHERE

There are many particle and electromagnetic radiations from the sun that eventually find their way to the ionosphere and below. This chapter will discuss just one, the energy transfer. This chapter will discuss the solar wind interaction with the magnetosphere and also the magnetospheric interaction with the ionosphere. This interaction is sometimes called coupling between the regions. A change in energy is just one of the causes of the constituent changes in the ionosphere and it will be discussed here in greater detail.

2.1 SOLAR WIND-MAGNETOSPHERIC COUPLING

The solar wind is basically a proton-electron gas that streams past the Earth with a mean velocity of 400 to 500 km per second and mean proton and electron density of about 5 per cubic centimeter [Tascione, 1988]. The solar wind interacts with the Earth's magnetic field, which in turn interacts with the ionosphere, causing changes to occur in the ionospheric region. Roughly 1% of the kinetic energy of the solar wind plasma impinging on the dayside magnetosphere is extracted by several different coupling processes. Solar wind energy enters the magnetosphere and drives all dynamic and steady state plasma processes in the Earth's magnetosphere and ionosphere before it is dissipated. The magnetopause coupling processes can be roughly divided into two categories. One category is the interaction between the solar wind magnetic field and the terrestrial field at the dayside magnetopause via field line merging. The other category is "non-magnetic" mechanisms which are usually referred to as quasi-viscous processes [Baumjohann, 1986]. It has been suggested by theoretical considerations, direct and indirect evidence, and laboratory experiments that magnetic merging is the dominant coupling process and provides roughly 90% of the energy input into the magnetosphere.

Once the solar wind enters the magnetosphere, the energy is intermediately stored and eventually dissipated as shown in Figures 1 and 2. Figure 1 shows the processes during a quiet time magnetosphere while Figure 2 shows the processes for a disturbed time magnetosphere. Part of the energy from the magnetosphere is transferred to the high-latitude ionosphere via field-aligned currents where it is dissipated by Joule heating. The other part of the energy is transferred to the magnetotail where it is intermediately stored as both plasma kinetic and thermal energy and magnetic field energy. Part of the magnetotail energy is then transferred to the ring current via particle injection where it is dissipated by charge exchange and subsequent loss to the earth atmosphere. Only a minor part of this magnetospheric energy is stored and transferred to the auroral ionosphere via (diffuse) precipitation. A second part of the magnetotail energy is transferred to the auroral ionosphere via particle precipitation and field-aligned currents where it is dissipated in the form of Joule heating (about 70%) and particle heating (roughly 30%) [Baumjohann, 1986]. The remaining part of the magnetotail energy is not dissipated within the magnetosphere but reenters the solar wind through the downtail release of plasmoids. There are two major sinks for solar energy in the magnetosphere. The more dominant one is probably the auroral ionosphere but a substantial part is also deposited in the ring current. A further investigation of the magnetospheric-ionospheric interaction and its processes is discussed in the next section.

2.2 MAGNETOSPHERIC-IONOSPHERIC COUPLING

As stated previously the magnetosphere is the result of the interaction of the solar wind with the Earth's magnetic field and particle populations. The interaction is complex, highly variable, and always present. A baseline magnetosphere is defined as that condition for which the magnetospheric energy content is minimum. Assuming the solar wind is the primary energy source for the magnetosphere, the baseline magnetosphere occurs when the


Total Energy Impinging on Magnetosphere	"Non-extracted" Energy		
	3.861x10 ¹³ W		
	Energy Extracted	Crosstail Input	Ring Current
		3x10 ¹¹ W	1.5x10 ¹⁰ W
			
		Polar Cap Input Birkeland Field- aligned Current Input	Precipitation Particles Auroral Region
4x10 ¹⁰ W			
Joule Heating			
1x10 ¹¹ W			
3.9x10 ¹³ W	3.9x10 ¹¹ W	1.4x10 ¹¹ W	

Figure 1. Process by which energy from the solar wind interacts with the magnetosphere and eventually exits the magnetosphere and heads for the ionosphere. The amount of energy "passed on" from one region to another is noted for each region. This figure represents quiet time conditions. Numerical values from Stern [1984].


Total Energy Impinging on Magnetosphere	"Non-extracted" Energy		
	3.861x10 ¹³ W		
	Energy Extracted	Crosstail Input	Ring Current
		3x10 ¹¹ W	2x10 ¹¹ W
			
		Polar Cap Input Birkeland Field- aligned Current Input	Precipitation Particles Auroral Region
			1x10 ¹¹ W
	Joule Heating		
			1x10 ¹¹ W
3.9x10 ¹³ W	3.9x10 ¹¹ W	2.7x10 ¹¹ W	

Figure 2. Exactly the same as Figure 1 except that this figure represents disturbed time conditions. Numerical values from Stern [1984].

solar wind energy coupling is minimized and when all previous energy inputs have been allowed to decay away [Gussenhoven, 1988]. Therefore it is important to know about baseline (quiet) conditions in the magnetosphere. Measured indicators of magnetospheric activity such as intensity and extent of large-scale current systems, auroral particle precipitation, and the cross-cap electric field potential can be used to identify when the quiet magnetosphere occurs and what its morphology is. From the magnetospheric baseline conditions, field-aligned currents can be looked at. Field-aligned currents are the way by which plasma motion perpendicular to the magnetic field is transmitted between the solar wind/magnetosphere and the ionosphere. The electric field distribution then results as a consequence of the coupling between the regions generating field-aligned current and the circuit constituted by the ionospheric conducting layer. Field-aligned currents are an important method of energy transport from the magnetosphere to the ionosphere, and will be looked at in more detail here.

2.3 FIELD-ALIGNED CURRENTS

Several definitions are found in literature to describe field-aligned currents. One definition is that field-aligned currents are the means by which the solar wind, magnetosphere, and ionosphere adjust their motions in such a way that in steady state, magnetic flux can be interchanged without accumulation at all heights [Caudal and Blanc, 1988]. Another interpretation is that field-aligned currents are an important aspect of magnetospheric dynamics because they provide a consistency check for descriptions of the electric and magnetic fields and the particle populations, because they directly couple the ionosphere to the magnetosphere and because their carriers can be the source of wave-generating instabilities and auroral arcs [Gussenhoven, 1988]. So, field-aligned currents are ultimately generated by the relative motion between the magnetosphere and the solar

wind and are the means by which the solar wind-magnetospheric dynamo is connected to the terrestrial ionosphere.

Field-aligned currents can be line currents (confined in both latitude and longitude), sheet currents (having a much smaller latitudinal than longitudinal extent), or global currents (broadly distributed in both latitude and longitude). There are three areas in which regularly occurring, large-scale, field-aligned current systems have been identified. These three areas correspond quite well with "accepted" regions in the ionosphere, the auroral region, the polar cusp region, and the polar cap region.

The main processes by which field-aligned currents are generated in the atmosphere are region 1 and region 2 currents. Region 1 currents are recognized to be produced primarily by the convective derivative of the plasma flow vorticity, resulting from the divergence of inertial currents produced by flow deceleration in the solar wind, due to its interaction with the Earth's magnetosphere [Caudal and Blanc, 1988]. They increase in intensity with increasing magnetic activity and, except for periods of highest activity, are stronger in the day sector than in the night sector [Gussenhoven, 1988]. Region 2 currents are believed to be produced essentially by pressure gradients built up in the region of closed field lines. This is due to the fact that in this region the thermal energy of energetic trapped particles is much larger than the kinetic energy of their drift across magnetic field lines. The electric field pattern is then established as a result of the coupling between the magnetospheric circuit and the circuit constituted by the ionospheric conducting layer [Caudal and Blanc, 1988]. Except in the near-midnight region during times of high magnetic activity, the region 2 currents have lesser intensity than region 1 currents and are correlated with the strengths of the ionospheric electrojets [Gussenhoven, 1988]. Since region 1 and region 2 currents have different variations with magnetic activity and have different spatial distributions, they are ascribed to different sources and driving mechanisms. While it is generally agreed that region 2 currents occur on closed field lines, the relationship of the

position of region 1 currents to the "last closed field line" and to the convection electric field reversal appears to vary greatly and indicate multiple drivers of the region 1 currents. These region 1 and region 2 currents are linked with the auroral region of the ionosphere and affect the happenings in the auroral region.

The second class of field-aligned currents is the cusp currents which may occur as sheet currents or line currents. Because the cusp currents are continuous to the dayside region 1/region 2 currents and because the variation in cusp current signatures is so great, there is still a great deal of uncertainty about their structure. Attempts to model the cusp currents using convection electric field patterns together with conductivity models usually produce significantly more complex cusp field-aligned current models than the empirical models. This field-aligned current is tied to the polar cusp region of the ionosphere.

It is also important to look at the field-aligned currents over the polar cap and in the region of closed magnetic field lines, the third class of field-aligned currents. Over the polar cap the antisunward plasma flow is set in response to the dawn-to-dusk electric field associated with the double sheet of region 1 currents. The flow lines tend to bend toward dawn, as a consequence of the day-night asymmetry of ionospheric conductivities. In the region of closed magnetic field lines a fundamental result is that pressure gradients can generate field-aligned currents only through their "azimuthal" component (where azimuthal refers to the component perpendicular to both the magnetic field and the gradient of the unit flux tube volume). At equilibrium, any plasma distribution should be azimuthal symmetric. The mere presence of an electric field in the magnetosphere produces a displacement of the population of energetic trapped particles, thus producing azimuthal pressure gradients, which constitute a first source for region 2 field-aligned currents. But azimuthal pressure gradients can also build up as a consequence of losses undergone by the plasma as it is azimuthally convected. Since those two processes for producing azimuthal pressure gradients drive field-aligned currents with different diurnal distributions, the

actual distribution of region 2 currents will result from a complex interplay of the two processes acting on both the ionic and electronic populations [Caudal and Blanc, 1988]. Studies on the variation of the polar cap potential with solar wind and activity parameters indicate that the weakest electrical coupling of the magnetosphere and the solar wind, for a given orientation of the IMF, occurs for minimum solar wind velocity and B after some specified $B(z)$ decay time. All are parameters which describe baseline conditions for the magnetosphere. Although currents do not play a direct role in F region ionospheric physics, they perhaps define boundaries, regions, electric fields, and auroral ovals in the ionosphere, hence they are ancillary but important. Now that the effects of the magnetosphere and solar wind have been looked at, it is time to consider the effects in the region called the thermosphere.

2.4 IONOSPHERIC-THERMOSPHERIC COUPLING

The ionosphere-thermosphere system also has a significant effect on the magnetosphere. Precipitating auroral electrons produce conductivity enhancements which can modify the convection electric field, large-scale current systems, and the electrodynamics of the magnetosphere-ionosphere system as a whole. Also, once the thermosphere is set in motion due to convection electric fields, the large inertia of the neutral atmosphere will act to produce dynamo electric fields whenever the magnetosphere tries to change its electrodynamic state. Additional feedback mechanisms occur on polar cap and auroral field lines via a direct flow of plasma from the ionosphere to the magnetosphere. In the polar cap, the continual outflow of thermal plasma from the ionosphere represents a significant source of mass, momentum, and energy for the magnetosphere. On auroral field lines, hot ionospheric plasma is injected into the magnetosphere via ion beams, conics, rings, and toroidal distribution [Schunk, 1988]. At

this time the thermosphere is not regarded as a major source of ionospheric effects due to the complicity of the ionospheric dynamics.

It has been shown in this chapter how the interactions of the various regions of the solar terrestrial arena work together to cause changes and occurrences in all regions, the solar wind, the magnetosphere, the ionosphere, and the thermosphere. The rest of this thesis will concentrate on the ionosphere and the electron density therein. It is important to remember that all of the processes discussed here have some effect on electron density in all regions of the ionosphere.

CHAPTER 3

IONOSPHERIC OBSERVATIONS AND MODEL COMPARISON PROCEDURES

There are several ways to observe (measure) the status of the ionosphere. There are also several ways to model what is expected in the ionosphere. Ideally, there should be similarities between the observations and the models so that by using models we may be able to forecast future ionospheric conditions successfully. A successful forecast must rely on an accurate depiction of the real time ionosphere, hence it is important to compare real time observations with models to see how well the available models perform. This chapter will describe the observations, models, and comparison methodology.

3.1 METHOD OF OBSERVATION

The observations used in this thesis to describe the ionosphere were from the *Dynamics Explorer 2* satellite. The *Dynamics Explorer* program was a program of the National Aeronautics and Space Administration (NASA) that was designed to study coupling of energy, electric currents, electric fields, and plasmas between the atmosphere, ionosphere, and magnetosphere [Hoffman et al., 1981]. Two satellites were used. One was for a higher orbit (magnetospheric) and one was for a lower orbit (ionospheric). It is this lower orbit satellite, *Dynamics Explorer 2* (DE-2), that was used for the observations of the ionosphere. The satellite flew from August 1981 through March 1983 and made 8574 polar orbits around the earth. The orbit of the DE-2 was 305 km at perigee and 1300 km at apogee. It had an inclination of 90 degrees and hence was polar with an orbital period of 101 minutes. The rate of change of latitude of perigee was -3.34 degrees per day with an initial perigee at 25 degrees south latitude at a local time of 0200 hours. The nominal lifetime of the spacecraft was 27.5 months and the pole to pole scan of perigee required less than two months. For neutral atmospheric measurements, orbital sectors near the

noon-midnight meridian over the polar region occurred at the beginning of the mission while dawn to dusk sectors occurred during winter months.

Instrumentation on board the DE-2 satellite measured magnetic fields, electric fields, neutral composition and density, components of the neutral wind, drift and temperatures of neutral and ionic atomic energy, components of ion drift normal to spacecraft velocity, thermal ion density, temperature irregularities, electron density, and ion and electron distributions to 30 keV [Hoffman et al., 1981]. Of these, the ion/electron densities and temperatures were used. This data is on microfiche here at Utah State University. Figures 3 and 4 show sample data from the microfiche. Ten minutes of data are shown in each panel and the full satellite ephemeris both geographically and geomagnetically is specified (see text scales at the bottom of Figures 3 and 4). The bottom panel shows the ion density and ion density fluctuation (only the ion density was used in this study), and the top panel shows the electron temperature. The date and orbit number are given at the top of the two panels. In addition, a polar plot of the satellite ground path is given. This is used to deduce which ionospheric regions were being crossed by the satellite, as well as determining the ascending node of this particular pass. Figure 3 shows sample data where a specific feature, a trough, is readily visible in the density panel at around $60^\circ\Lambda$ (invariant latitude). This figure is for the part of the orbit descending away from the north pole. In Figure 4, the ionosphere is less structured than in Figure 3. There is no obvious density feature although an electron temperature enhancement in the cusp region is present. This is a part of an orbit that passes over the north pole from $74.22^\circ\Lambda$ ascending through $70.74^\circ\Lambda$ descending, which is shown here.

3.2 LIMITATIONS OF DATA

Although the satellite does give global coverage over its lifetime, there are still limitations on data coverage which give information that is other than what might ideally be expected.

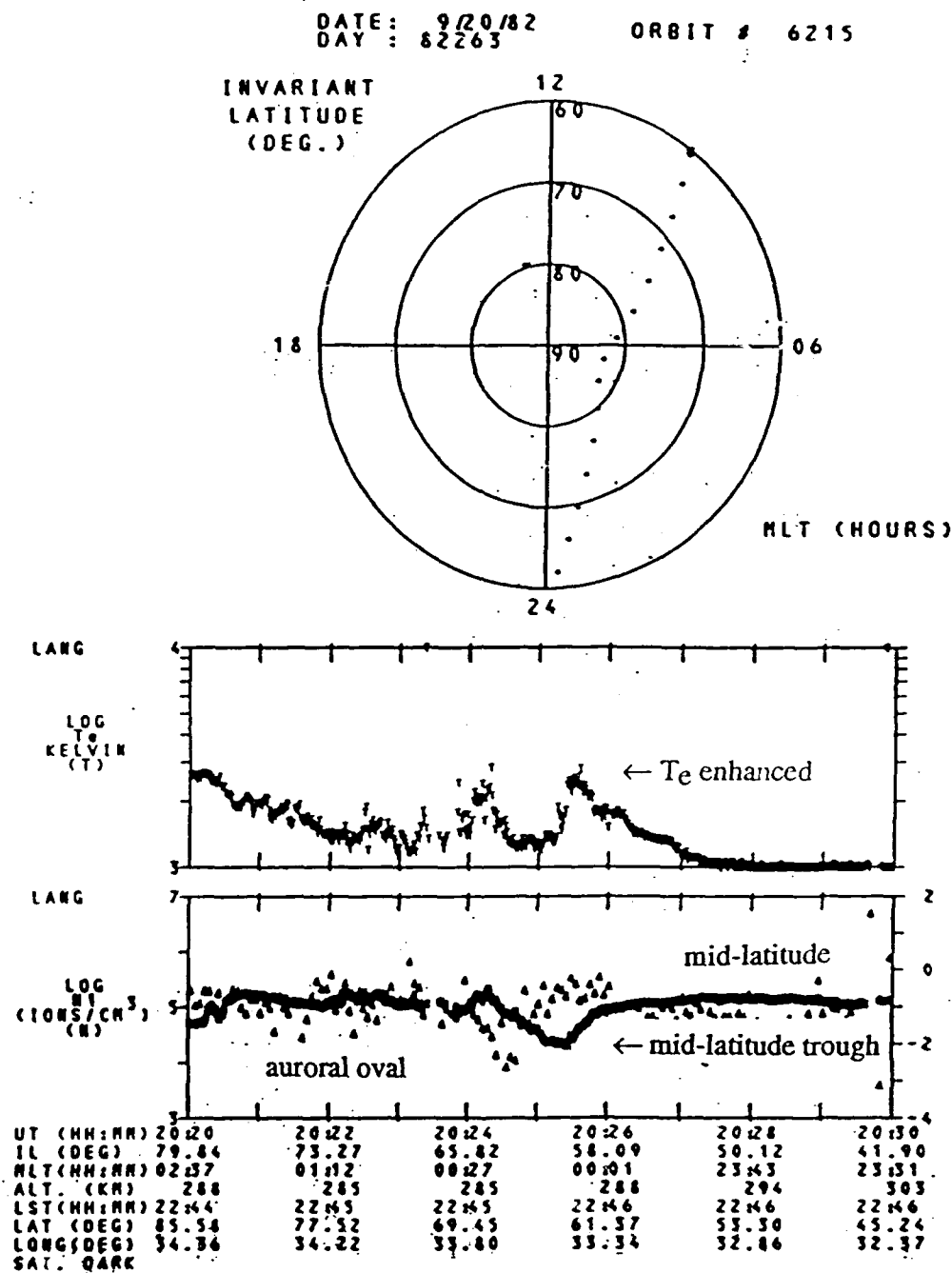


Figure 3. Sample data from the DE-2 microfiche showing data for September 20, 1982, orbit number 6215. This figure shows a well defined trough in the region of 60°A. This is a descending part of the orbit from 79.84° through 41.90°A. The polar plot at the top shows the satellite's ground path to aid in determining which regions were being crossed by the satellite. The points in the bottom panel are the fractional change in ion density ($\Delta N_i/N_i$). The values are on the right axis in the bottom panel.

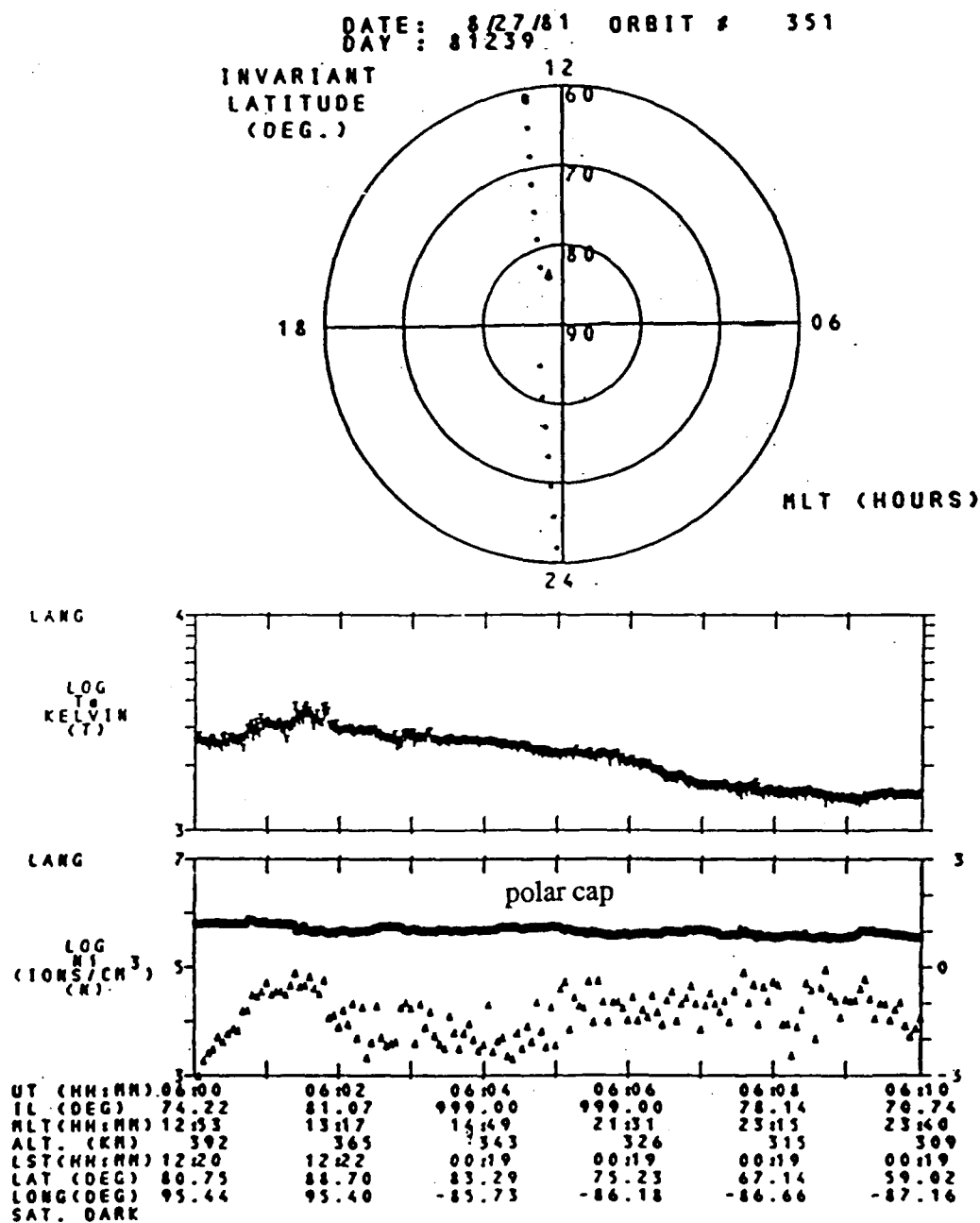


Figure 4. Same as Figure 3 except data is for August 27, 1981, orbit number 351. Here on the part of the curve from 74.22° ascending through 70.74° and descending the curve is less structured than in Figure 3.

One of these is the fact that the mission took place during solar maximum conditions. Table 1 lists the monthly averages of the sunspot number and Kp during the DE-2 lifetime. The sunspot averages lie between 50.1 and 169.3, showing that the DE-2 mission was carried out during solar maximum conditions. Hence, this study is biased to these conditions and differences which may occur during solar minimum cannot be addressed directly. In this study Kp values greater than or equal to 4.0 are referred to as high Kp, or high geomagnetic activity. All other values (less than 4.0) are referred to as low Kp, or low geomagnetic activity. Figure 5 shows a graph of magnetic local time (MLT) through which the spacecraft passed on any given day as the satellite crosses 50°N going poleward in the northern hemisphere. This is limiting in the fact that something may be occurring outside this orbit local time which cannot be observed by the instruments on board the satellite. Adding approximately 12 hours to these given in Figure 5 would give the MLT as the satellite leaves the northern high latitude ionosphere.

Models exist that try to reproduce the ionosphere. No model is able to reproduce the ionosphere under all conditions, i.e., region, level of solar or geomagnetic activity, season. Two models were used to compare to the DE-2 data. One, the International Reference Ionosphere (IRI), is an empirical, global model. The other, the Time Dependent Ionospheric Model (TDIM), is a physical, regional model. In this application the TDIM inputs restricted comparisons to magnetic latitudes greater than 50 degrees. Because of this regional aspect, and due to the fact that most geomagnetic effects are not directly felt below 50 degrees, the concentration will be on the 50 to 90 degree region for both models and DE-2 observations. After a brief description of both models, the methodology used to compare these models with the DE-2 data will follow.

Table 1. The listing of average monthly Kp's and Sunspot Numbers

MONTH/YEAR		AVERAGE Kp	AVERAGE SUNSPOT NUMBER
AUG	1981	3.0	158.2
SEP	1981	2.7	169.3
OCT	1981	3.7	161.2
NOV	1981	3.0	135.6
DEC	1981	2.3	147.1
JAN	1982	2.7	110.7
FEB	1982	4.3	162.6
MAR	1982	3.3	153.7
APR	1982	3.7	122.5
MAY	1982	3.3	81.4
JUN	1982	3.7	110.4
JUL	1982	4.3	102.6
AUG	1982	3.7	105.9
SEP	1982	4.7	119.2
OCT	1982	3.3	94.3
NOV	1982	3.7	98.5
DEC	1982	3.7	126.4
JAN	1983	3.0	85.8
FEB	1983	4.0	50.1

3.3 INTERNATIONAL REFERENCE IONOSPHERE

The IRI was developed by K. Rawer and others [Brown et al., 1991]. The model serves as a standard reference for various purposes such as design of experiments, estimation of environmental and other effects, and for testing theories. The model summarizes the experimental data from rockets and satellites to provide true height profiles of the ionosphere. The IRI is based on 13 standard CCIR parameters obtained from ionosondes, incoherent scatter radar, satellites, and rocket observations. It may also use URSI parameters scaled from ionosondes to provide an average ionospheric density profile [Jursa, 1985]. The model provides information about ion and electron density and ion composition. It calculates the plasma density profiles from 50 to 2000 km for every hour, and produces plasma density profiles, electron and ion temperature profiles, and percentage

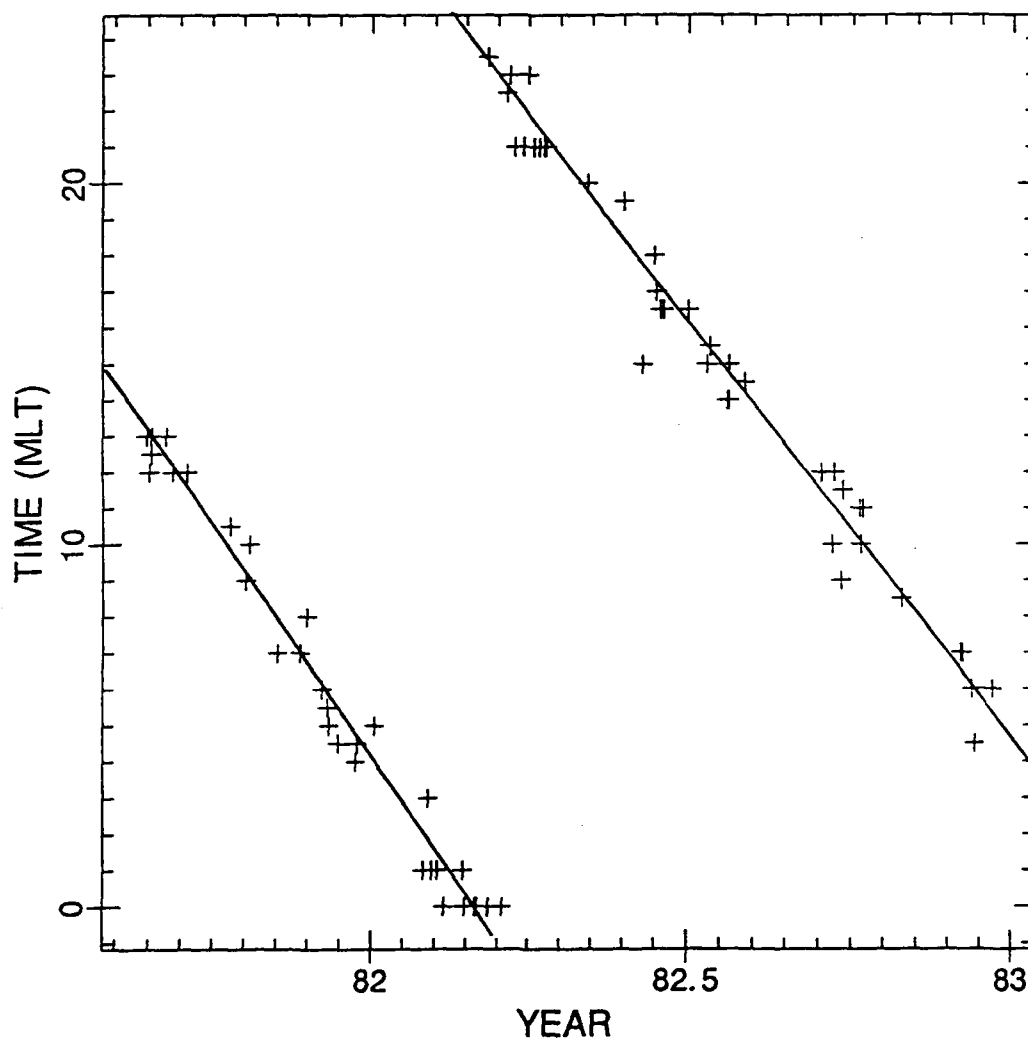


Figure 5. A plot of the orbits of DE-2 satellite. On any given day, the start time of the orbit at $50^{\circ}\Lambda$ is plotted. The orbit then would be from 50° ascending across the pole and out at 50° descending at approximately 12 hours after start time. About year 82.164, the orbit would be midnight-noon. A noon-midnight orbit occurs around year 82.671. Dawn to dusk passes take place at 3 different times throughout the DE-2 mission.

of ion compositions. The inputs to this model include latitude and longitude (geographic or geomagnetic) for specific solar activity (sunspot number or F10.7 cm flux). The month, day, and time (local or universal) are also required. Because this is an empirical model, a model which relies on real data, and despite the fact that most of the data stations are ground-based below 50 degrees latitude, the IRI takes this data and uses it for global calculations. So, it may be giving false or inaccurate information for regions outside the observing locations. This includes the region greater than 50 degrees, which is the area we are looking at. Despite this, people still use the IRI to model this region. So while it is a "global" model, the input data that it uses is only from regions that are extensive at mid and low latitudes and sparse at high latitudes.

3.4 TIME DEPENDENT IONOSPHERIC MODEL

The TDIM is a computer model which numerically solves the F-region continuity and momentum equations for ions and the F-region energy equation for both ions and electrons [Schunk, 1988, Sojka, 1989]. It is a physical model which gives a climatological representation of mid to high latitudes (30 to 90 degrees) based on solar conditions, season, geomagnetic activity, and IMF. Several inputs are required to solve the various equations. These include auroral precipitation, convective E field, heat flux, extreme ultraviolet from the sun, neutral atmosphere, MSIS, and the neutral wind. The TDIM has been run for a series of climatological conditions to create an ionospheric data base. To extract data from the model data base the geomagnetic latitude, geomagnetic local time, universal time, altitude, and species of ions desired, solar cycle, Kp, and the B(y) component of the IMF are also required. The 108 data sets that were created by the model are for diurnally reproducible conditions, for the conditions indicated in Table 2. This model data base is also the basis for the PRISM (Parameterized Real-time Ionospheric Specification Model) model used by the Air Force.

Table 2. TDIM climatology data base conditions

<u>PARAMETER</u>	<u>NAME</u>	<u>SPECIFIC CONDITIONS</u>
F10.7	solar activity	70, 130, 210
Kp	geomagnetic activity	1, 3+, 6
ap	geomagnetic activity	4, 18, 80
day	season	82, 173, 357
By	IMF By (assumed south)	negative, positive
hemisphere	hemisphere	north, south

3.5 DATA VERSUS MODEL COMPARISONS

In the data versus model comparisons, a comparison of electron density between the models and observations will be done because changes that occur in the ionosphere by different events ultimately cause changes in density. Changes in temperature, electric field, auroral precipitation, incoming solar flux all cause the ion density to change. These changes are due to the dependence of ion production, ion loss (recombination) and diffusion on these parameters. Thus measuring (observing) electron densities is a practical method to measure (observe) changes in ionospheric regions. For these comparisons, a statistically reasonable sample of orbits (88 cases) will be used. These will be selected to have a reasonable distribution over season, IMF (northward and southward), and geomagnetic activity. Each orbit will be critically compared rather than simply carrying out an average over all 88 orbits.

There has been a lot of discussion on the ionospheric dependence upon northward (positive values) and southward (negative values) direction of IMF. These differences stem from the convection pattern that results from the different IMF directions. The southward direction appears to be less ambiguous (a two cell pattern) in its structure so most studies have been carried out for this direction. More understanding of structure that

occurs during northward IMF conditions needs to be obtained. Each of these conditions occurs about 50% of the time. So, initially two sets of data exist, one for northward IMF and one for southward IMF.

For each of these conditions, varying Kp's were chosen that were characterized as either high or low. A Kp value of 4.0 was used as the criterion for designating an orbit as high or low. Kp is an index used to measure the intensity of magnetic disturbances in the mid to high latitude region. Varying levels of geomagnetic activity (Kp) play an important part in ionospheric changes. Each of the four IMF-Kp categories was divided into the four seasons since solar control of the ionosphere is also significant. From the 16 categories of data described above, both a qualitative and statistical comparison for each of the 88 related orbits will be done.

The key features to be compared include the various regions of the ionosphere. They are the polar cap region, the area from $80^{\circ}\Lambda$ to the north pole, the auroral region, the area between $65^{\circ}\Lambda$ and $80^{\circ}\Lambda$, the mid-latitude region, and the region of mid-latitude troughs. These last two regions are from about $50^{\circ}\Lambda$ to $65^{\circ}\Lambda$. Here a comparison can be done to see if the features in these regions are comparable between the observations and the models. Also to be looked at is whether the models pick up the observed features or in some instances do the models depict features which are not observed. Tables 3 and 4 list the orbits that were analyzed along with the day the orbit occurred, the season, the sunspot number (SSN), as well as the Kp. Table 3 is for north IMF conditions, while Table 4 is for south IMF conditions. Methods of comparisons and results of actual comparisons follow in the next chapter.

Table 3. Data from northward IMF

ORBIT	DAY	SEASON	SSN	Kp	H/L *
302	81235	AUTUMN	200	6.0	H
309	81236	AUTUMN	178	2.7	L
344	81238	AUTUMN	215	2.3	L
357	81239	AUTUMN	222	5.3	H
527	81251	AUTUMN	208	2.3	L
556	81253	AUTUMN	196	2.0	L
686	81262	AUTUMN	156	5.0	H
2095	81356	WINTER	75	0.7	L
2102	81357	WINTER	86	1.7	L
2249	82002	WINTER	94	1.7	L
2298	82005	WINTER	112	0.7	L
2668	82030	WINTER	211	5.3	H
2719	82033	WINTER	241	5.7	H
2856	82042	SPRING	158	4.3	H
3125	82060	SPRING	168	7.0	H
3240	82068	SPRING	116	2.3	L
3370	82076	SPRING	180	4.0	H
3396	82078	SPRING	167	1.0	L
3466	82083	SPRING	122	2.0	L
3545	82088	SPRING	169	1.3	L
3591	82091	SPRING	145	4.0	H
3743	82101	SPRING	152	4.7	H
4171	82129	SUMMER	47	1.3	L
4232	82133	SUMMER	78	2.0	L
4426	82146	SUMMER	117	5.0	H
4587	82157	SUMMER	108	4.0	H
4771	82169	SUMMER	134	1.0	L
5169	82195	SUMMER	222	6.0	H
5303	82204	SUMMER	74	1.7	L
5326	82205	SUMMER	27	6.0	H
6116	82257	AUTUMN	104	1.3	L
6215	82263	AUTUMN	104	2.3	L
6224	82264	AUTUMN	102	5.7	H
6292	82268	AUTUMN	118	4.3	H
6440	82278	AUTUMN	109	2.3	L
7319	82335	WINTER	88	0.0	L
7335	82336	WINTER	125	0.3	L
7466	82344	WINTER	166	5.3	H
7614	82354	WINTER	63	4.3	H
7662	82357	WINTER	96	2.0	L

* H means high Kp (values greater than 4.0). L means low Kp (values less than 4.0)

Table 4. Data from southward IMF

ORBIT	DAY	SEASON	SSN	Kp	H/L
327	81237	AUTUMN	189	3.7	L
351	81239	AUTUMN	222	1.7	L
471	81247	AUTUMN	170	2.3	L
647	81259	AUTUMN	138	2.0	L
837	81272	AUTUMN	191	1.3	L
1016	81284	AUTUMN	131	5.7	H
1154	81293	AUTUMN	183	6.7	H
1181	81295	AUTUMN	145	5.0	H
1423	81311	WINTER	192	2.5	L
1488	81316	WINTER	160	6.4	H
1614	81324	WINTER	82	3.0	L
1626	81325	WINTER	82	2.7	L
1669	81328	WINTER	59	2.0	L
1813	81337	WINTER	212	2.3	L
1852	81340	WINTER	234	0.3	L
1872	81341	WINTER	244	2.0	L
1945	81346	WINTER	240	4.0	H
2386	82011	WINTER	46	0.7	L
2746	82035	WINTER	221	5.0	H
2796	82038	SPRING	226	3.3	L
3024	82053	SPRING	100	6.3	H
3033	82054	SPRING	97	3.0	L
3133	82061	SPRING	174	7.7	H
3223	82067	SPRING	140	1.7	L
3428	82080	SPRING	153	4.7	H
3630	82094	SPRING	137	4.0	H
3676	82097	SPRING	130	1.7	L
3728	82100	SPRING	138	6.3	H
4025	82120	SPRING	79	4.7	H
4106	82125	SPRING	63	3.0	L
4128	82127	SPRING	69	1.5	L
4698	82164	SUMMER	139	6.3	H
4709	82165	SUMMER	137	4.0	H
4741	82167	SUMMER	128	2.0	L
4759	82168	SUMMER	136	2.3	L
4986	82183	SUMMER	41	2.0	L
5021	82185	SUMMER	42	0.3	L
5137	82193	SUMMER	187	5.0	H
5316	82205	SUMMER	27	5.0	H
5458	82214	SUMMER	68	5.3	H
6245	82265	AUTUMN	95	5.3	H
6300	82269	AUTUMN	138	5.7	H
6450	82279	AUTUMN	55	3.3	L
6469	82280	AUTUMN	54	4.7	H
6811	82302	AUTUMN	101	4.7	H
7214	82328	WINTER	96	7.3	H
7433	82342	WINTER	184	4.3	H

CHAPTER 4

OBSERVATIONS VERSUS MODEL COMPARISONS

In order to be able to compare observations and models, a preliminary step of actually selecting a subset of observations must first be undertaken. The first part of this chapter will describe the criteria for choosing the observations. The second part of the chapter will talk about comparison techniques and actual comparison results from the observations and models. These first comparisons are average results based on statistical and qualitative comparisons.

4.1 CHOOSING ORBITS FOR ANALYSIS

The first thing that was done was to look at the IMF data from NSSDC data base which covered the entire DE-2 mission time frame. Initially only the northward IMF data was examined. This direction occurs around 50% of the time so there are many potential orbits (about 4287). The criterion of positive values of the IMF was used to mean northward direction. We have this data in hourly values. Orbits that occurred after several hours of northward IMF were looked for to be sure that the northward condition was "established." This was also done as much as possible with the IMF B(y) and Kp indices as well. This goal was not always achievable, however. The actual value (intensity) of the northward IMF did not matter, just the mere fact that it was positive. Initially, winter and summer conditions only were looked at during orbits of high Kp (values of greater than or equal to 4.0) and low Kp (values less than 4.0). An attempt was made to vary the Kp somewhat in these categories, i.e., for high Kp some 5's and some 6's were used and for low Kp some 1's and some 2's were used. Values on either side of 4.0 for each category were also used. The data search for orbits was later extended to include both the spring and autumn seasons as well. The placing of days in their actual season was done by taking an equal number of days before and after the equinox or solstice days. For example, my spring

began about 45 days before the vernal equinox. The data was spread out over the entire season instead of lumping all the data around the same day or days.

Initially around 8 to 11 orbits were targeted for each region, which includes IMF direction, season, and Kp. Table 5 shows the actual number of orbits that had usable data from the targeted number for each region. This is the first place where the DE-2 fiche data was actually used. As can be seen from the table, the number of orbits at the end was not the number targeted. The number in the table represents the number of orbits where data was found that met the above criteria. Questions may be raised as to whether the number of orbits chosen is statistically sufficient. If trends could be noted using the above figures, then it is doubtful that more data for each region would reveal new or significantly different trends. Also, if no trend is noted it is also unlikely that more data would lead to a definite trend being detected. Some of the reasons that some perspective orbits from the DE-2 fiche were not usable were that in some cases data was missing entirely from the fiche (all that appeared were blank "boxes"). Another reason was that only partial orbits existed. Some partial orbits were chosen where more than half of the orbit was present and an extremely high or low Kp value was noted. An effort was made to keep partial orbits to a minimum. Another reason density data was not used from the fiche data was that data existed but it was outside the 50° to 90° latitude that was required to compare with the models. A fourth problem was that in some cases the hours (orbits) of interest were not on the fiche. In other words there were gaps in the data on some days. Another reason was that on very rare occasions data existed for an appropriate orbit but not in the parameter that was being looked at (i.e., the density panel).

From the data that was deemed "acceptable" the IRI and TDIM models were run individually, using the necessary parameters (day, year, Kp, F10.7, sunspot number, universal time, altitude) depending on the requirements for each model, to obtain density values at each two-minute interval as taken from appropriate fiche data. The two-minute

Table 5. Breakout of observations by Kp values and seasons

	Northward IMF		Southward IMF *	
	Hi Kp	Lo Kp	Hi Kp	Lo Kp
EQUINOX	5	4	6(8)	6(8)
SUMMER	4	4	5(8)	4(8)
EQUINOX	5	7	7(9)	6(11)
WINTER	4	8	5(10)	8(10)
	<u>18</u>	<u>23</u>	<u>23(35)</u>	<u>24(37)</u>

* The value in parenthesis was the number of orbits looked for, not all had data.

time interval was chosen for the simple fact that ephemeris data existed on the DE-2 fiche for two-minute intervals. The DE-2 fiche takes data every five seconds so with the two-minute interval, there were 24 observation points being recorded. The two-minute interval would be enough to give increasing or decreasing density trends in the orbit but may not have depicted the exact location of the extreme minimum or maximum. Electron density values were chosen because the ionosphere is affected by the geomagnetic activity, electric fields, currents, convection patterns, etc. all of which have an effect on the electron density in the ionosphere. Ultimately, there were three density values for each point, one the DE-2 observation, one from the IRI and one from the TDIM. The rest of the orbit was done until all ephemeris points had values for the entire orbit of interest. These points were then plotted on the same graph (time vs. density). For all three models (IRI, TDIM, and DE-2) analysis and comparison of the resulting "curves" that were formed when the various densities from the same source were connected were achieved.

4.2 EXAMPLE OF CURVE COMPARISONS

One initial thing to look at on the graph is the comparison between the model curve and the observation curve and to how well the model detected features (maximum or minimum

densities) that were seen in the observations. This gives an initial idea as to whether there is agreement between models and observations. Ideally it is hoped that all three curves would be on top of each other. In the cases looked at, however, this never happened.

Some criteria that could be looked at to compare are (using the DE-2 data as basis for comparison) whether the model curves have the same general shape throughout. In other words, whether electron density trends (increasing or decreasing) were consistent with the observations and whether features seen in the observations were detected in the model. If the models depict a feature, whether the feature shows up at the exact time of observed feature or before or after the observed feature is used for comparison as well. Also to be looked at is whether the models depict a feature which the observation says does not exist. Figures 6 through 9 show examples of four different orbits with DE-2, TDIM, and IRI orbit curves on them. In each figure the octagon-shaped symbols are the DE-2 observations, the plus sign symbols are the TDIM curve, and the diamond-shaped symbols are the IRI curve. Figure 6 shows an example of agreement in the TDIM curve but not the IRI. Figure 7 shows an example of agreement in the IRI curve but not the TDIM curve. The example in Figure 7 is an exception as shall be shown later. Figures 8 and 9 show examples of poor agreement in both models. It is these two figures which the majority of graphs resemble.

4.3 STATISTICAL COMPARISON

The simplest and most obvious comparison is a statistical comparison between models and observations. For each point a percentage value was calculated by subtracting the model density value from the observation density value and dividing by the observation density value and multiplying by one hundred to get percent. Taking all the values in one orbit, adding them together, and then taking the average (total + number of points) gave an average percentage for the entire orbit. Each orbit in each IMF direction, in each season,

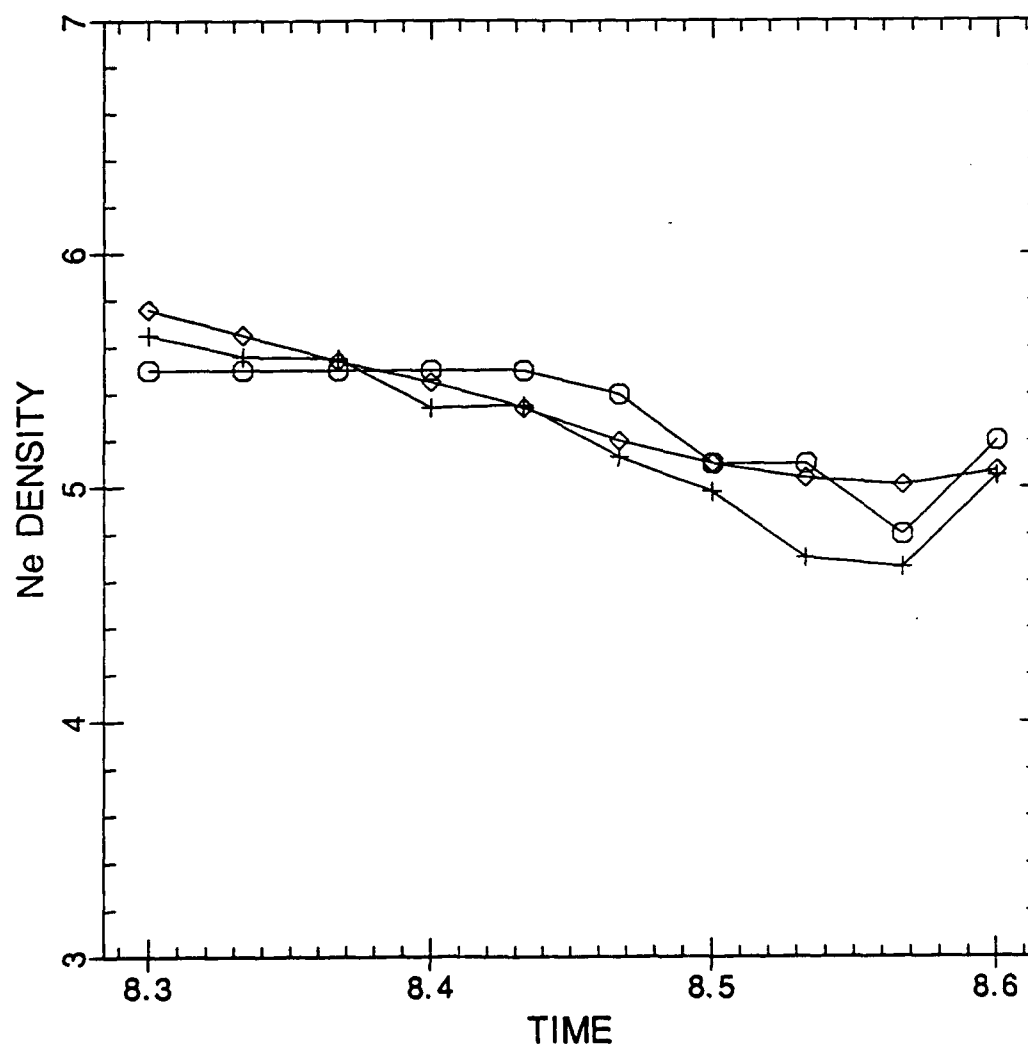


Figure 6. This figure shows an example of agreement between the TDIM curve (plus sign symbol) and the observations (octagon-shaped symbol). Notice that the general features that are observed are discernible in the TDIM model curve. The rest of the curve has favorable comparison also. The features are a lot less discernible in the IRI curve (diamond-shaped symbols).

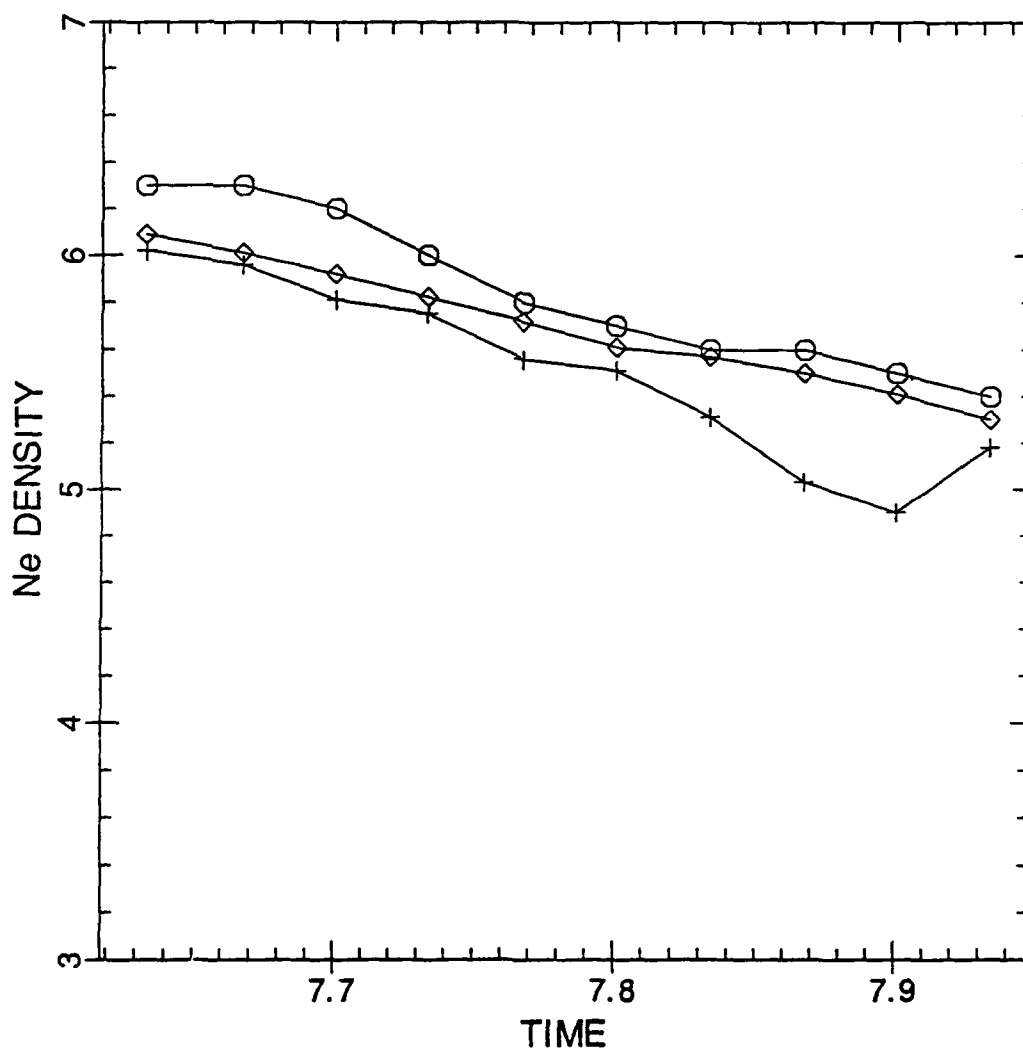


Figure 7. This figure shows an example of good agreement between the IRI and the observations. Here the general trend and shape are basically the same between the IRI model and the observations. The TDIM curve does show a tendency toward the same trend but depicts a feature late in the orbit that the observation does not depict.

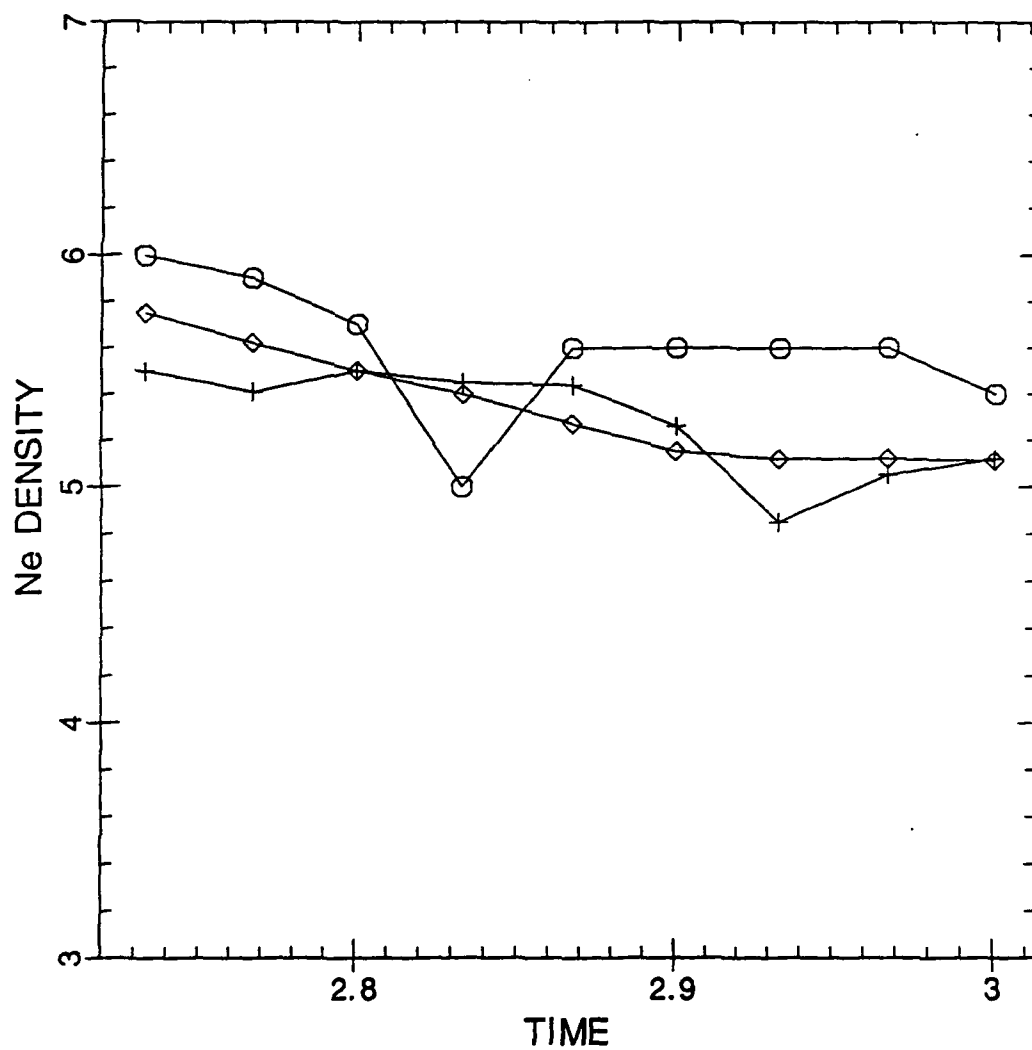


Figure 8. An example of a case where neither IRI nor TDIM model agrees with the observed curve at all.

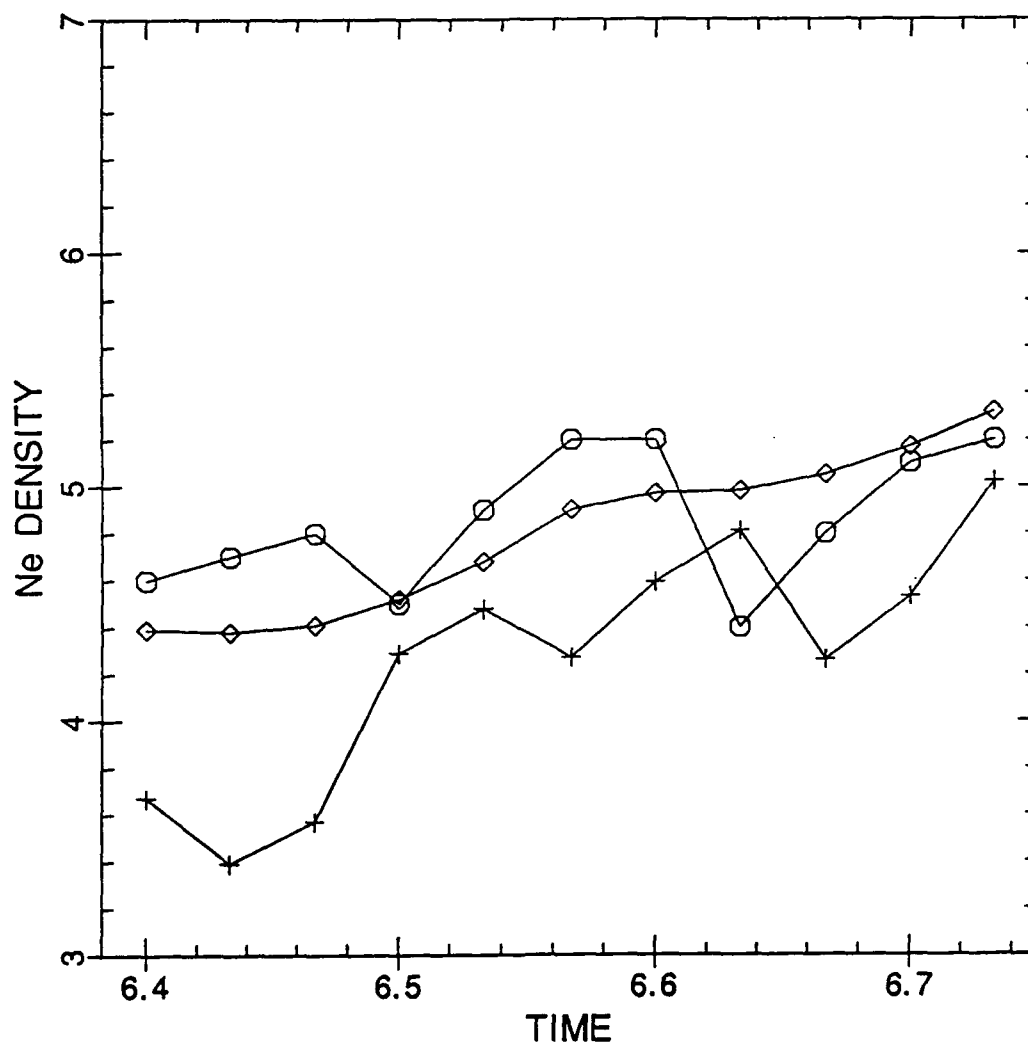


Figure 9. Another example of no agreement between the models and the observations. All or part of most graphs resemble both of these last 2 figures.

and each Kp were done the same way and added together to give an overall average value for each condition as shown in Table 6. It can be seen from the table that overall the TDIM has an average difference of 10.4% for all conditions. It appears to do a slightly better job for overall northward IMF conditions than the southward direction. It should be pointed out that the TDIM model overestimates values during periods of high Kp and underestimates values during periods of low Kp. Hence a low percentage difference overall is attained. The IRI percentage from the table is much worse than the TDIM with a percentage difference of -78.5%. This model appears to do a little better job in the southward IMF condition but it is still much worse than the TDIM model. Table 7 shows standard deviation average for each condition. This was done by taking the standard deviation between the model and the observations at each point and averaging over the entire orbit for each season just as in the percentage calculation. From this table it can be seen that the standard deviation for the TDIM model is less than that for the IRI model with both models showing better results in the southward IMF condition as opposed to northward. It is now time to examine the qualitative aspects of the curve comparisons.

4.4 QUALITATIVE COMPARISONS

For each orbit a "rating" system was used with the ratings of excellent, good, fair, and poor being used to describe the orbits. An excellent rating had curves with almost exact agreement including the magnitudes of the curves. A good rating was one in which most of the curve agreed with the observation. In this condition, the model must detect features (area of maximum or minimum densities) that are observed. A fair rating had some agreement in the curves. Here the model may or may not have detected the observed features. A poor rating implied little or no agreement between models and observations. Figure 10 shows a rough sketch of two model curves and an observation curve with appropriate rating system given to the model's curves for clarification of the rating system.

Table 6. Statistical average difference between observations and models

<u>SEASON</u>	<u>NUMBER OF ORBITS</u>	<u>TDIM</u>	<u>IRI</u>
NORTHWARD IMF			
HI Kp			
SPRING	5	-6.8%	-159.7%
SUMMER	4	5.5%	-130.3%
AUTUMN	5	-55.7%	-129.6%
WINTER	4	-37.4%	-332.7%
AVERAGE:	18	-24.5%	-183.3%
LOW Kp			
SPRING	4	23.3%	-19.2%
SUMMER	4	45.4%	10.1%
AUTUMN	7	13.0%	-43.9%
WINTER	8	44.9%	-70.9%
AVERAGE:	23	31.5%	-39.6%
AVERAGE NORTH:	41	6.9%	-102.7%
SOUTHWARD IMF			
HI Kp			
SPRING	6	-49.2%	-101.5%
SUMMER	5	-5.8%	-28.6%
AUTUMN	7	-16.9%	-134.4%
WINTER	5	24.3%	-144.1%
AVERAGE:	23	-14.0%	-104.9%
LOW Kp			
SPRING	6	32.2%	-37.1%
SUMMER	4	23.4%	1.6%
AUTUMN	6	29.1%	-14.8%
WINTER	8	61.0%	2.8%
AVERAGE:	24	39.5%	-11.8%
AVERAGE SOUTH:	47	13.4%	-57.4%
AVERAGE ALL:	88	10.4%	-78.5%

Table 7. Standard deviation average difference between observations and models

<u>SEASON</u>	<u>NUMBER OF ORBITS</u>	<u>TDIM</u>	<u>IRI</u>
NORTHWARD IMF			
HI Kp			
SPRING	5	65.8%	131.6%
SUMMER	4	42.8%	117.0%
AUTUMN	5	143.4%	154.3%
WINTER	4	148.8%	290.2%
AVERAGE:	18	100.7%	169.9%
LOW Kp			
SPRING	4	43.4%	48.2%
SUMMER	4	15.7%	16.4%
AUTUMN	7	49.4%	48.3%
WINTER	8	33.4%	107.4%
AVERAGE:	23	36.9%	63.3%
AVERAGE NORTH:	41	64.9%	110.1%
SOUTHWARD IMF			
HI Kp			
SPRING	6	113.9%	116.6%
SUMMER	5	48.9%	33.4%
AUTUMN	7	70.7%	142.4%
WINTER	5	57.4%	152.7%
AVERAGE:	23	74.3%	114.2%
LOW Kp			
SPRING	6	31.6%	50.9%
SUMMER	4	20.6%	20.9%
AUTUMN	6	35.5%	52.2%
WINTER	8	33.8%	62.4%
AVERAGE:	24	31.5%	50.0%
AVERAGE SOUTH:	47	52.5%	81.4%
AVERAGE ALL:	88	58.3%	94.5%

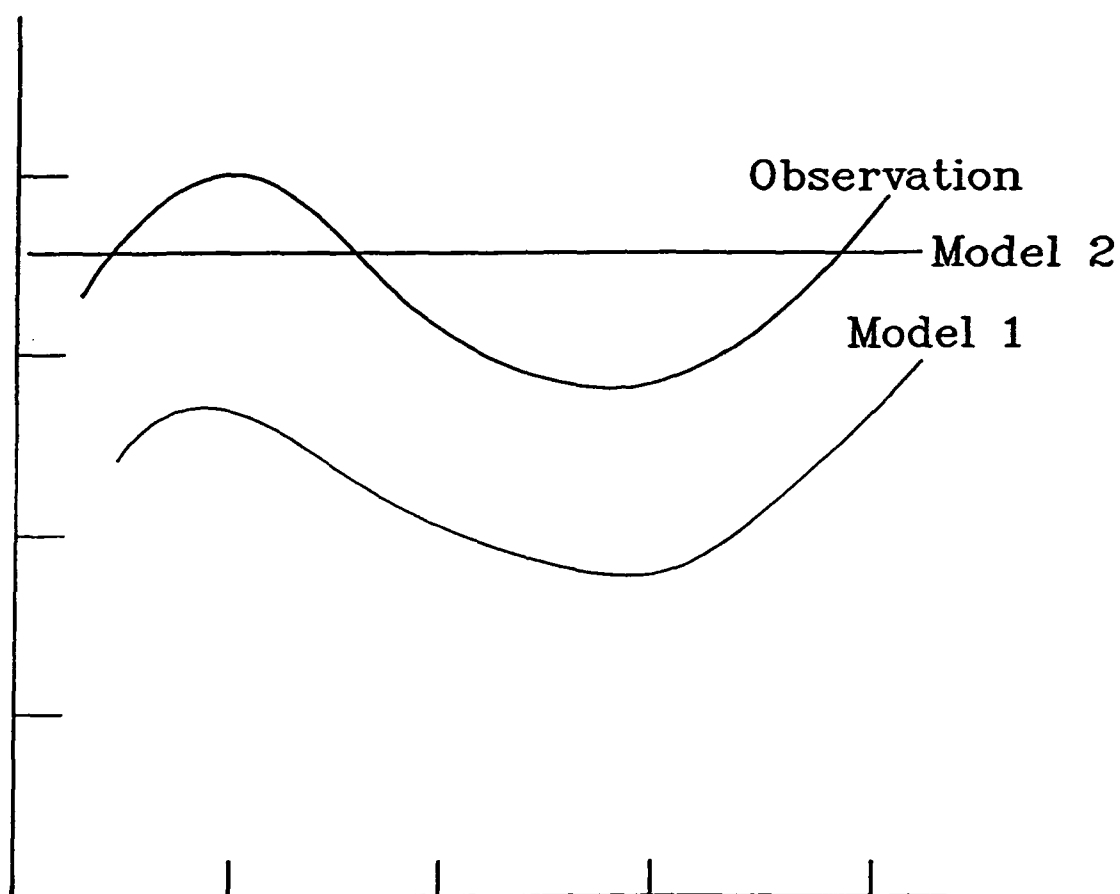


Figure 10. Clarification of definition of terms. In this graph, model number 1 would be given a good rating because the shape and magnitude (intensity) are consistent. Whereas model number 2 would be poor because even though it might have the same magnitude as the observations curve, the shape of the model curve shows no features at all.

For help in comparing the curves a numerical percentage range was assigned to each rating. Excellent ratings had average curve agreement of 80 to 100%. Good ratings had an average curve agreement of 60 to 80%. Fair had an average of 40 to 60% and poor had less than 40% agreement in the curve comparisons. Averaging these results over all the orbits by IMF direction, season, and Kp, over all the orbits, gives the results in Table 8. As can be seen from the table, the averages are fair at best. This implies that the curves overall have no better agreement than 60% and most cases are around 40 to 45%. The IRI continually rated a poor because the model does not detect the structure that is occurring in the ionosphere. Since the ionosphere is almost always structured somewhere, the IRI model would never depict that and would therefore give a poor representation. So from here on, any comparisons between models and observations will be for the TDIM only.

4.5 OTHER INTERPRETATIONS OF THE CURVES

To add credence to the subjectivity of these results, three other opinions were sought comparing these curves. Their results are shown in Tables 9 through 11. Table 9 gives results from an expert in the field while the other two tables are from people with little or no experience dealing with the ionosphere. The criteria the other people used were exactly the same as the criteria that were used in Table 8. However, the expert used density trends instead of features in his curve comparisons. As can be seen from Tables 8 through 11, there is variability between people and their interpretation of the curves. It is seen, however, that in all cases the IRI did no better than the TDIM and in most cases and most conditions it did worse than the TDIM. It is also interesting to note that the expert's comparisons were consistently better (higher percentage of agreement) than the three non-experts. So, as stated previously, since the IRI does not "model" for features, it will be ignored for the duration of this thesis. The next chapter will discuss actual analysis of the data and some conclusions that can be drawn from the data.

Table 8. Qualitative difference between observations and models

<u>SEASON</u>	<u>NUMBER OF ORBITS</u>	<u>TDIM</u>	<u>IRI</u>
NORTHWARD IMF			
HI Kp			
SPRING	5	F	P
SUMMER	4	F	P
AUTUMN	5	F	P
WINTER	4	F	P
AVERAGE:	18	F	P
LOW Kp			
SPRING	4	P	P
SUMMER	4	F	P
AUTUMN	7	P	P
WINTER	8	F	P
AVERAGE:	23	F	P
AVERAGE NORTH:	41	F	P
SOUTHWARD IMF			
HI Kp			
SPRING	6	P	P
SUMMER	5	F	P
AUTUMN	7	F	P
WINTER	5	F	P
AVERAGE:	23	F	P
LOW Kp			
SPRING	6	F	P
SUMMER	4	F	P
AUTUMN	6	F	P
WINTER	8	F	P
AVERAGE:	24	F	P
AVERAGE SOUTH:	47	F	P
AVERAGE ALL:	88	F	P

Table 9. Qualitative difference between observations and models

<u>SEASON</u>	<u>NUMBER OF ORBITS</u>	<u>TDIM</u>	<u>IRI</u>
NORTHWARD IMF			
HI Kp			
SPRING	5	G	F
SUMMER	4	F	F
AUTUMN	5	G	F
WINTER	4	G	P
AVERAGE:	18	G	F
LOW Kp			
SPRING	4	G	G
SUMMER	4	G	G
AUTUMN	7	G	G
WINTER	8	F	G
AVERAGE:	23	G	G
AVERAGE NORTH:	41	G	F
SOUTHWARD IMF			
HI Kp			
SPRING	6	G	F
SUMMER	5	G	F
AUTUMN	7	G	F
WINTER	5	G	F
AVERAGE:	23	G	F
LOW Kp			
SPRING	6	G	G
SUMMER	4	G	G
AUTUMN	6	G	G
WINTER	8	G	G
AVERAGE:	24	G	G
AVERAGE SOUTH:	47	G	G
AVERAGE ALL:	88	G	F

Table 10. Qualitative difference between observations and models

SEASON	NUMBER OF ORBITS	TDIM	IRI
NORTHWARD IMF			
HI Kp			
SPRING	5	P	P
SUMMER	4	P	P
AUTUMN	5	F	P
WINTER	4	P	P
AVERAGE:	18	P	P
LOW Kp			
SPRING	4	P	G
SUMMER	4	P	F
AUTUMN	7	F	P
WINTER	8	P	P
AVERAGE:	23	P	F
AVERAGE NORTH:	41	P	P
SOUTHWARD IMF			
HI Kp			
SPRING	6	F	P
SUMMER	5	F	P
AUTUMN	7	F	P
WINTER	5	F	P
AVERAGE:	23	F	P
LOW Kp			
SPRING	6	P	P
SUMMER	4	P	F
AUTUMN	6	F	F
WINTER	8	P	P
AVERAGE:	24	P	F
AVERAGE SOUTH:	47	P	P
AVERAGE ALL:	88	P	P

Table 11. Qualitative difference between observations and models

SEASON	NUMBER OF ORBITS	TDIM	IRI
NORTHWARD IMF			
HI Kp			
SPRING	5	F	F
SUMMER	4	F	F
AUTUMN	5	F	F
WINTER	4	P	P
AVERAGE:	18	F	F
LOW Kp			
SPRING	4	F	F
SUMMER	4	F	F
AUTUMN	7	F	F
WINTER	8	F	F
AVERAGE:	23	F	F
AVERAGE NORTH:	41	F	F
SOUTHWARD IMF			
HI Kp			
SPRING	6	F	F
SUMMER	5	G	F
AUTUMN	7	F	F
WINTER	5	F	F
AVERAGE:	23	F	F
LOW Kp			
SPRING	6	F	G
SUMMER	4	G	G
AUTUMN	6	F	G
WINTER	8	F	F
AVERAGE:	24	F	F
AVERAGE SOUTH:	47	F	F
AVERAGE ALL:	88	F	F

CHAPTER 5

ANALYSIS OF DATA

At each data point the invariant latitude was used that corresponded to that point from the DE-2 data. This latitude would help in placing the orbit in its appropriate region of the ionosphere (polar cap, auroral oval, mid-latitude, or trough). Density maximums or "relative" density maximums were used for all regions except the trough region where minimum or "relative" minimum density trends were used. Once again, the actual density value did not matter but the trend (increasing or decreasing) in values did. So by using the above criteria, appropriate latitude range, appropriate density trend, and in some cases using the electron temperature panel for assistance, each curve was placed into a region. Some curves were not readily put into a region. They could have easily fit into more than one region or there was no obvious "fit" at all. These curves were put into a separate category called "not well defined." In each region the data was grouped together by IMF, season, and Kp for possible future comparisons among similar parameters. This whole procedure was repeated for southward IMF conditions. This chapter will describe each region individually and tell some of the results of analysis and conclusions for each region and for the model compared with the observations overall.

5.1 TROUGH REGION

The first region to be discussed is the trough region. A trough is an area of minimum electron densities from about 50° to 65° A. It is primarily a *nightside phenomenon*, extending in a band from the dusk sector to the dawn sector [Moffett and Quegan, 1983]. Troughs are most frequently observed when the solar zenith angle is greater than 90° degrees. Troughs have been observed in the noon sector as well. They are most regularly observed during winter and equinox. In the summer they are only observed near local midnight. The poleward edge of the trough, usually seen as a sharp increase in electron

concentration, lies just equatorward of the boundary of diffuse auroral precipitation. The poleward edge of the trough is usually steeper than the equatorial edge. It was found from the occurrences of troughs in this thesis study that this was true only about 38.7% of the time. The rest of the cases had the equatorward edge steeper or no obvious difference in steepness was observed. Figure 11 shows the aurora relative to the plasma convection paths. Here the trough would lie equatorward of the auroral (shaded) region. It is also seen that the latitude of the trough decreases through the night. At quiet times there may be movement back towards higher latitudes in the dawn sector. During periods of increased magnetic activity, the trough tends to move to lower latitudes. The occurrence of the trough and the validity of the previously mentioned points do not depend markedly on solar cycle variations. There is currently no consensus from the field on the width or depth of the trough, or the local time of the deepest point [Moffett and Quegan, 1983].

There are several physical factors or processes that affect troughs. They are as follows in relative order of importance. First is plasma convection. This causes a stagnation point around 1800 MLT with slow eastward flow on the nightside from dusk through midnight toward dawn [Moffett and Quegan, 1983]. This feature is noted in Figure 11. The second process is ion chemistry, which is defined by how the rate of reaction of atomic oxygen varies. An increase in ion temperature may lead to an increase in the rate coefficient of reaction. It is noted from the cases studied here that an increase in electron temperature coincided with an occurrence of a trough about 79% of the time. The other 21% had either no change or a decreasing electron temperature. The third factor that affects troughs is auroral tendency. The aurora defines the poleward boundary of the trough. Also, the poleward or equatorward movement of the aurora, and thus the movement of the troughs, by an increase or decrease in electric fields, particle precipitation, etc., can help in detecting trough movement poleward or equatorward. The fourth factor is plasma escape. Here plasma escapes along magnetic field lines by the upward flow of hydrogen in the polar

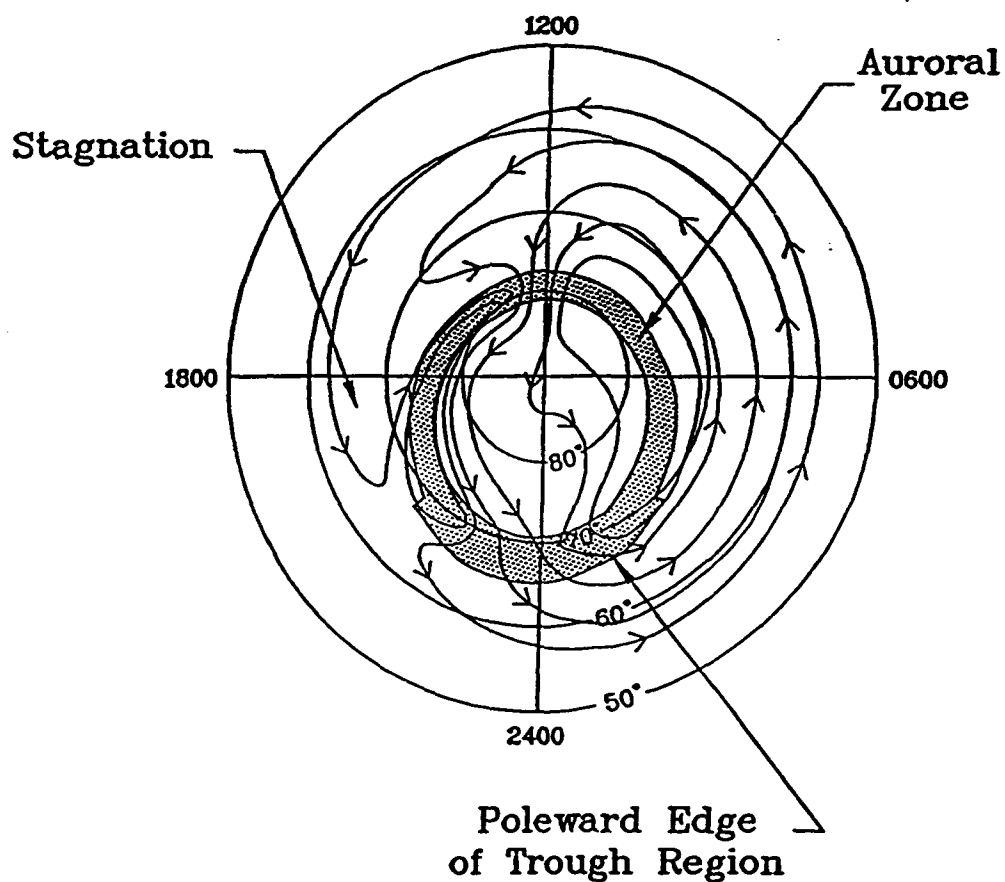


Figure 11. This figure shows the plasma convection paths as well as the position of the auroral oval. The mid-latitude trough lies equatorward of this auroral region boundary. One cause of trough formation is the stagnation region which this figure also shows in the vicinity of 1800 MLT.

wind acts to decrease the oxygen content and contributes to the rate of decay of the F-layer. This is dependent on whether closed or open plasmasphere field lines exist. For closed field lines it will be a nighttime mechanism and a loss mechanism. In combination with other processes, this may account for part of the ionization depression in the trough. The last factor to be addressed is that of neutral winds. Here the raising or lowering of the F-region by these neutral winds causes decreased or increased decay rates. Also the relative ion-neutral velocity determines the ion temperature in F-region and the winds may transport vibrationally excited nitrogen into the trough region.

It has been shown here what troughs are and what factors affect the trough so the modeling of the region by the TDIM will be examined here. Figure 12 shows an example of relatively good agreement between the TDIM and the DE-2 observations. Here the trough feature is observed at $57.58^\circ\Lambda$. The TDIM also depicts a trough here but the commencement of the trough is depicted earlier in the model than what is observed. Table 12 shows results of observation versus the TDIM model for the trough region during both northward and southward IMF conditions. It is important to note here that some troughs may have appeared on the DE-2 fiche which were not used in this data. This is because the data at two-minute intervals was used as shown on the fiche data. It is possible that troughs fell in between these two-minute sectors and therefore did not get analyzed. Since the average movement of the satellite during these two minutes was about 7° latitude, or about 700 km, this would imply that these troughs could be considered as insignificant when all the orbits are compared. Figure 13 shows an example of relatively poor agreement between the TDIM model and the DE-2 observations. This figure shows a trough occurring at $60.47^\circ\Lambda$ on the descending orbit. The TDIM shows a trough in this region but it is not nearly the magnitude (intensity) of the observed. Also the DE-2 curve shows a density increase earlier in the orbit which is not depicted in the TDIM curve. It has been shown here how bad the model is. The question is how can it be improved to

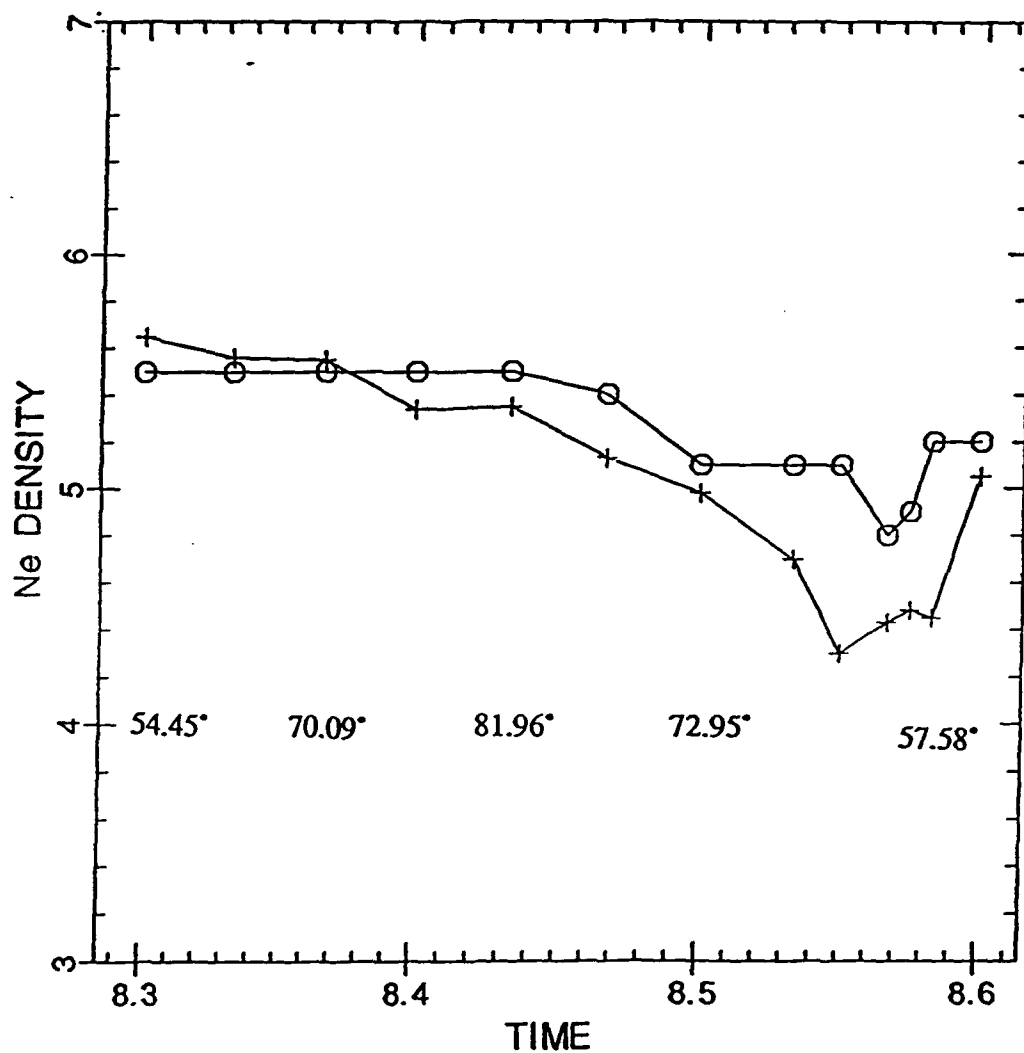


Figure 12. This figure shows relatively good agreement between the TDIM and the DE-2 observations. A trough is observed around 57.58°A on the descending orbit. The TDIM shows a trough occurring in the same general area just before the observed trough in the orbit. The rest of the curve compares well with the observation curve.

Table 12. Specifications of the trough region

	IMF NORTHWARD	IMF SOUTHWARD	TOTAL
Feature evident in model:			
	12/14 (85.7%)	4/11 (36.4%)	16/25 (64.0%)
Feature showed up:			
BEFORE	4/14 (28.6%)	1/11 (9.1%)	5/25 (20.0%)
EXACTLY	6/14 (42.9%)	3/11 (27.3%)	9/25 (36.0%)
AFTER	2/14 (14.3%)	0/11 (0.0%)	2/25 (8.0%)
N/A	2/14 (14.3%)	7/11 (63.6%)	9/25 (36.0%)
Magnitude of feature:			
GREATER	1/14 (7.1%)	1/11 (9.1%)	2/25 (8.0%)
EQUAL TO	2/14 (14.3%)	1/11 (9.1%)	3/25 (12.0%)
LESS THAN	9/14 (64.3%)	2/11 (18.2%)	11/25 (44.0%)
N/A	2/14 (14.3%)	7/11 (63.6%)	9/25 (36.0%)

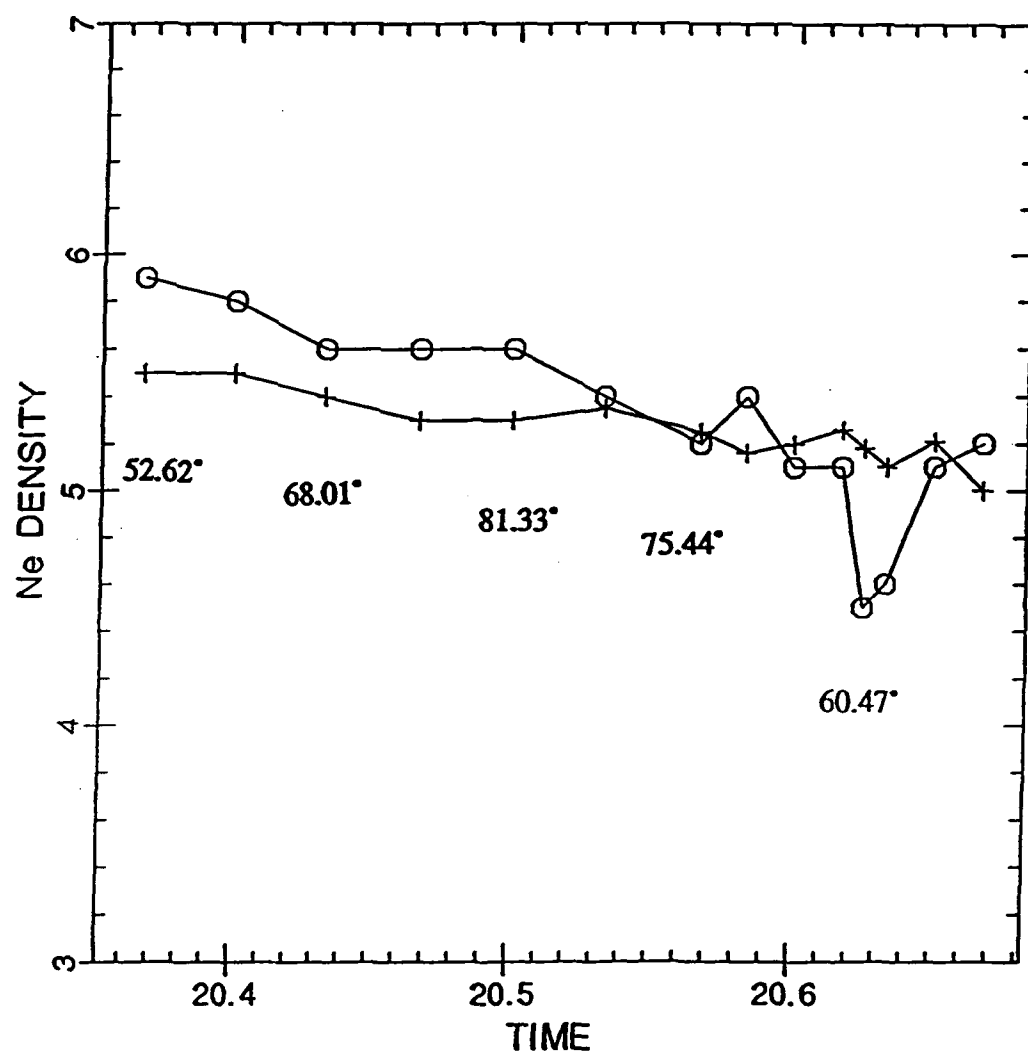


Figure 13. This is a figure where the model and the observations are not in very good agreement. While the TDIM does appear to detect the trough in the region of 60.47°\AA , it is not nearly as deep as the observed trough. The TDIM shows this minimum density to be occurring slightly later than the observed. Also, the observations show a density maximum at about 70°\AA which the model does not detect. The rest of the curve shows some agreement with the observations.

make it acceptable with the observations and maybe even to be able to forecast from this. In order to make an acceptable forecast, a first "initial" position of the trough must first be established. First it should be pointed out that the disagreement exists because the model does not handle the instantaneous convection properly since it uses a statistical pattern and therefore the stagnation part of the trough is not successful. If it were possible to input information from a location of a "known" trough, i.e., electric field, auroral inputs, ion/electron temperatures in the known trough region, and composition of the ionosphere in the trough region, and assuming a trough exists horizontally around the world, the TDIM should be able to show a trough at an initial position since the model does extend to other local times. These mentioned parameters plus particle precipitation in the aurora and the actual "monitoring" of the auroral oval by remote sensing can give preliminary indications as to the poleward edge of the trough and therefore movement of the trough.

Therefore, if the model has an indication of where the present trough exists, the following parameters are what need to be measured or monitored to aid in forecasting the location of the trough in the future. The real trough particle composition and densities need to be looked at. Also, the electric fields and trends of the electric fields (increasing or decreasing) would help in forecasting. Particle precipitation is a third parameter to be measured to determine if more or less energy is being put into the system. Geomagnetic activity is an important thing to measure but it must be done on a much more enhanced scale than is currently capable of being done. Köhnlein and Raitt [1977] suggest that using geomagnetic activity would give much more useful data. Using the equation

$$\Lambda = 65.2 - 2.1K_p - 0.5t \pm 2^\circ \quad (1)$$

where K_p is the geomagnetic activity and t is the time of day, helps to establish the trough location. Currently geomagnetic data is available in three hourly increments. A much smaller time frame of K_p should be used to achieve a much more accurate position and

forecast. Another parameter to be considered is the ion/electron temperature. Of these parameters, the in situ ones are less important than the others because they are occurring at the time of the trough so very little forecasting would be useful. The important thing to be considered is the time that elapses between these other changes in parameters and the actual formation (movement) of the trough, or perhaps the change in intensity (increasing or decreasing) of these parameters is what needs to be considered for forecasting future trough occurrences.

5.2 POLAR CAP REGION

Another region of the ionosphere with definable features is the polar cap region. The region covers the area from roughly $80^\circ\Lambda$ to the pole ($90^\circ\Lambda$). Generally the polar cap is relatively quiet but there are some exceptions. Atomic oxygen is generally the dominant ion at all altitudes of this region [Jursa, 1985]. One factor that occurs in the polar cap region which causes disturbances is varying geomagnetic activity. During periods of low geomagnetic periods, a wide range of ion compositions can occur in the polar F-region at different locations and times [Sojka et al., 1991]. In the summer hemisphere, the auroral precipitation associated with the low geomagnetic activity conditions is insufficient to create a marked density feature. During high geomagnetic activity higher electric fields induce upward plasma drifts in the dayside polar cap while in the nightside polar cap they induce downward drifts. This is just the opposite of quiet periods when the neutral wind-induced vertical drifts are dominant [Sojka, 1989]. Occasionally, particles diffusing out of the polar region escape into the magnetotail region from which some may become energized. This is known as polar wind and has mostly H^+ , He^+ , and O^+ as constituents [Jursa, 1985].

There are a few polar cap features which are seen during northward IMF or southward IMF conditions in the polar cap region. Two of these, tongues of ionization and patches of

ionization, are somewhat related. During southward IMF conditions, antisunward convection takes place over the polar cap region. This results in a tongue of ionization being formed. Under certain conditions, this tongue is "broken down" into "patches" of ionization. There are a few conditions for these patches. One is that they are UT dependent. They also depend on previous convective history. They are dependent on the $B(y)$ component of the IMF. An increase in cross-tail potential seems to help patches form. Patches originate equatorward of the cusp region. They are not related to any enhanced soft particle precipitation and therefore are not produced locally [Buchau et al., 1985], which implies advection into the region.

Anderson et al. [1988] suggest that creating and organizing polar cap patches are a result of a time-varying convective pattern. Figure 14 shows an example of a tongue of ionization as determined from the DE-2 plot. Figure 15 shows the TDIM model plot for the exact same time as Figure 14 with the tongue of ionization noted. From all the DE-2 data that was analyzed it was noted that the data does verify that tongues of ionization do indeed occur during southward IMF conditions as all of the occurrences in the data were southward and none were northward. In the 16 southward IMF orbits that were placed in the polar cap region, 11 showed examples of a tongue of ionization (about 68.8%). There were very few orbits from the other regions which showed tongues of ionization. Also noted was that whenever a tongue of ionization was observed, there was either an electron temperature decrease or no change at all in the electron temperature. Some things to look for (consider) in patches of ionization include a southward IMF, an increase in cross-tail potential energy, time varying convective pattern, and season (which implies how much time the plasma is in the sunlit region). Also to be considered are the electron temperature (for reasons stated above) and the electron density because one signature of the tongue of ionization is a density increase across the polar region. As in the trough region, these last two measurements are occurring at the same time and therefore would be adequate for

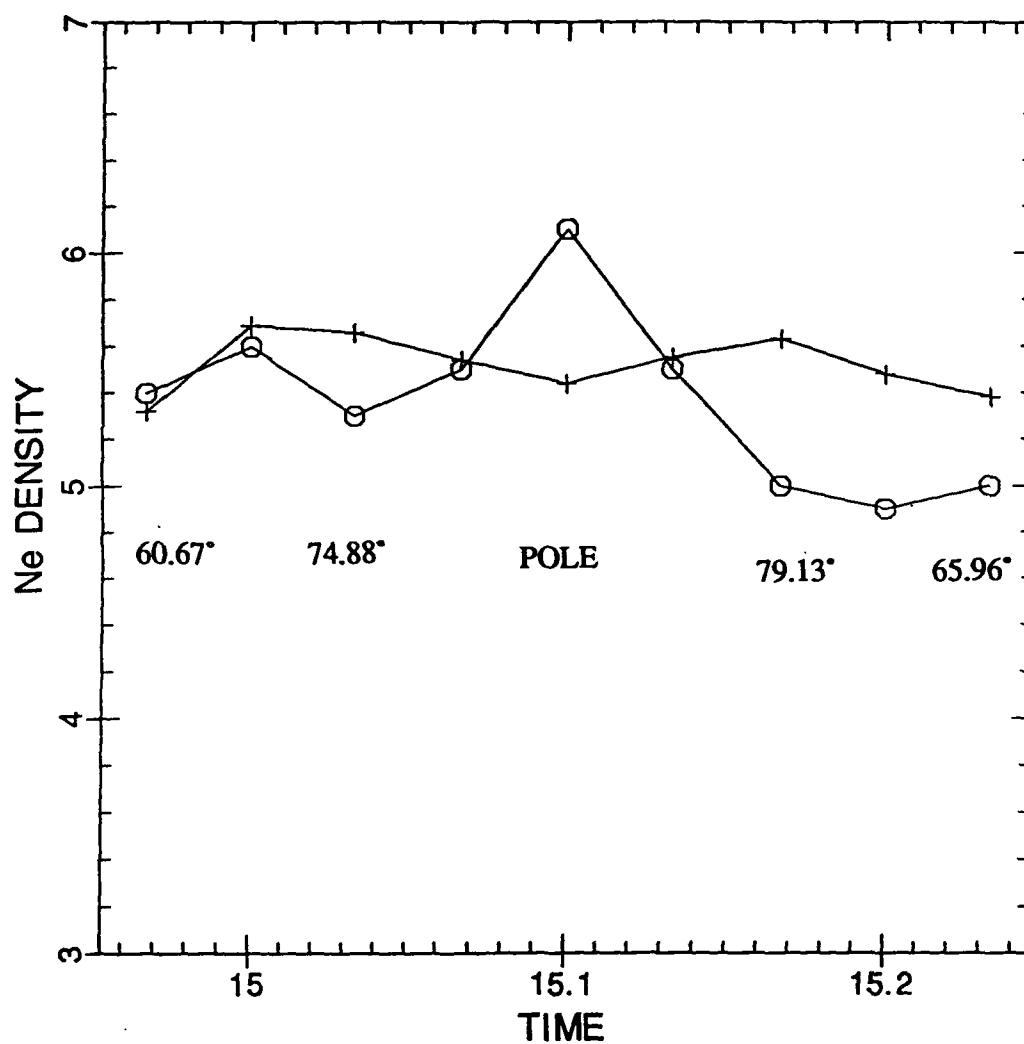


Figure 14. An example of a tongue of ionization from the DE-2 data. A significant density maximum is seen over the polar region at time 15.1. Due to the orbit of the DE-2 satellite, the tongue of ionization on the TDIM plot shown in Figure 15 for the same time frame did not get detected.

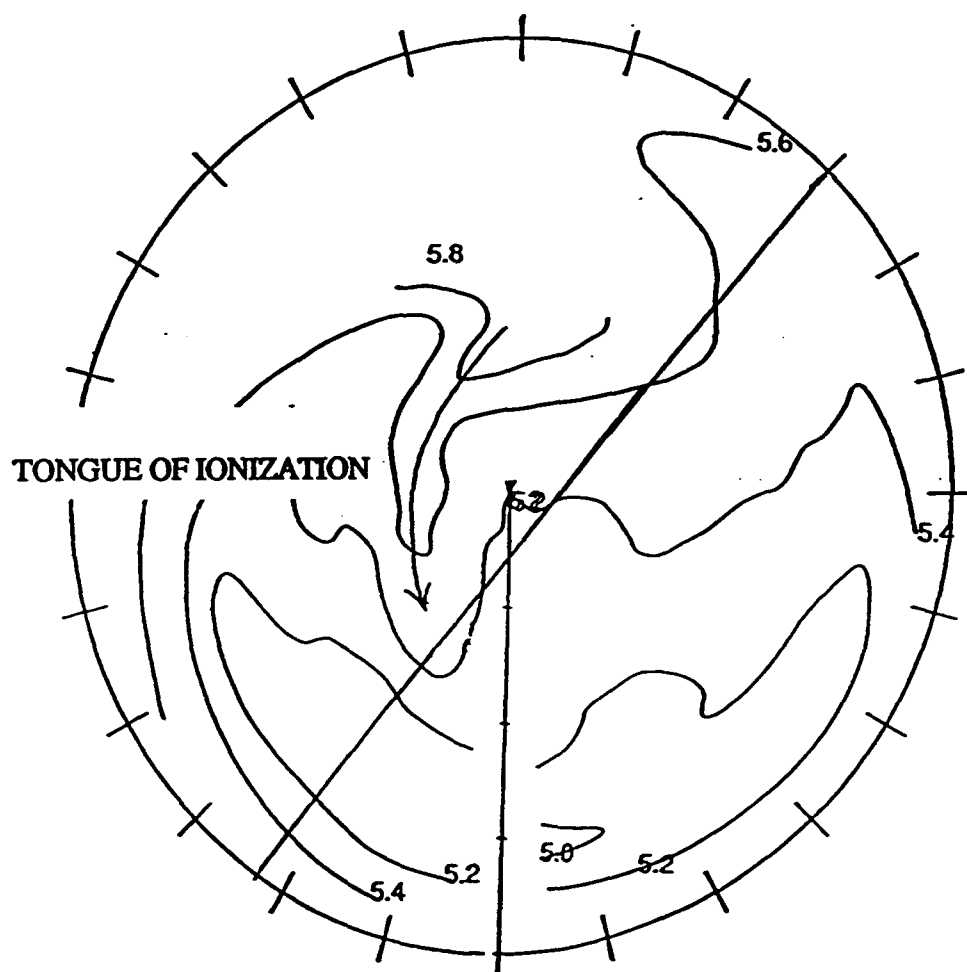


Figure 15. The TDIM model plot showing the tongue of ionization. The superimposed line is that of the DE-2 orbit. Note that it did not pass directly through the tongue and therefore was not detected.

placing the tongue of ionization in its present location but may not be helpful for forecasting future occurrences of tongues of ionization. Due to the size and method of formation of the tongue region, it usually takes on the order of hours for this feature to disappear.

Another feature which is readily seen in the polar cap region is that of sun-aligned arcs. These occur during low geomagnetic activity [Niciejewski et al., 1989]. They also occur during northward IMF conditions and are mainly seen during winter. Arcs are usually produced by soft electrons (<1 keV). Intense polar cap arcs are the optical signature of upward Birkeland currents associated with corresponding velocity gradient. There is some general consensus that some sun-aligned arcs are formed in a region of closed field lines with precipitating electrons having the characteristics of plasma sheet or plasma sheet boundary layer electrons [Valladares and Carlson, 1991]. Parameters that can be observed in sun-aligned arcs include electron density, electron/ion temperature, and plasma line-of-sight velocities. These parameters can be used to derive currents and fluxes in the arcs. This feature was not readily obvious from the fiche data used.

When a sun-aligned arc extends completely across the polar cap from the dayside to nightside sector of the auroral oval, a feature called the theta aurora is formed [Frank et al., 1986]. It is so called because when observed from above it resembles the Greek symbol theta (Θ). It tends to occur for strong northward IMF that is maintained over a period of time. Salient features of the theta aurora include the presence of precipitating ions accompanying the energetic electrons (>1 keV), its location in the region of sunward convection and possible existence of four cells of plasma convection [Valladares and Carlson, 1991]. This is not seen in the fiche data used. Theta auroras do not occur often due to the stringent requirements for their formation (strong northward IMF, strong electric fields, etc.) and are not detectable in the fiche data used in this study. Both sun-aligned

arcs and theta auroras are something that can be observed and thus can be put into a model for initialization.

Another feature that is seen in the polar cap region is polar holes. They are noted during times of weak convection and precipitation and are seen mostly in winter. They are seen in both the northward and southward IMF conditions. The morphologies of this effect are extremely hard to figure out. The regions are also not stationary for the most part. No continuing monitoring is possible (especially where the solar cycle (F10.7), magnetic activity (Kp) and diurnal (UT) dependencies all control the phenomena) [Sojka et al., 1991]. In the northern hemisphere, the polar hole is deepest in the 0500 - 0700 UT period and is least evident in the 1700 - 1900 UT period. Sojka [1989] found that during low geomagnetic activity, the level of ion production in the morning sector of the auroral oval has an appreciable effect on the location and spatial extent of the polar hole. During high geomagnetic activity, the polar hole results from large downward transport velocities that exist in the region. Sojka et al. [1991] also found from using the TDIM model that the northern polar hole is located in the postmidnight sector for $B(y)$ positive, while it is premidnight for $B(y)$ negative. Based on these extreme $B(y)$ values, the polar hole is deduced to lie between 2100 and 0300 MLT just poleward of the auroral oval [Sojka et al., 1991]. This particular feature would require monitoring up to hours beforehand to note any changes that might indicate a hole is present. This feature may or may not be discernible in the DE-2 fiche because of the polar hole's limited locations and limited times of occurrence. Unless the satellite orbit was actually passing through the region, the polar holes would not be detected. Figure 16 shows an example of a polar hole occurrence from the DE-2 observations. Figure 17 shows a polar hole occurring in the TDIM (shaded region) for the same time frame as the DE-2 curve in Figure 16. Parameters that can be looked at to locate a polar hole include MLT, electron density, and transport velocity of particles. Due to limitations on time of occurrences and location (MLT) of occurrences,

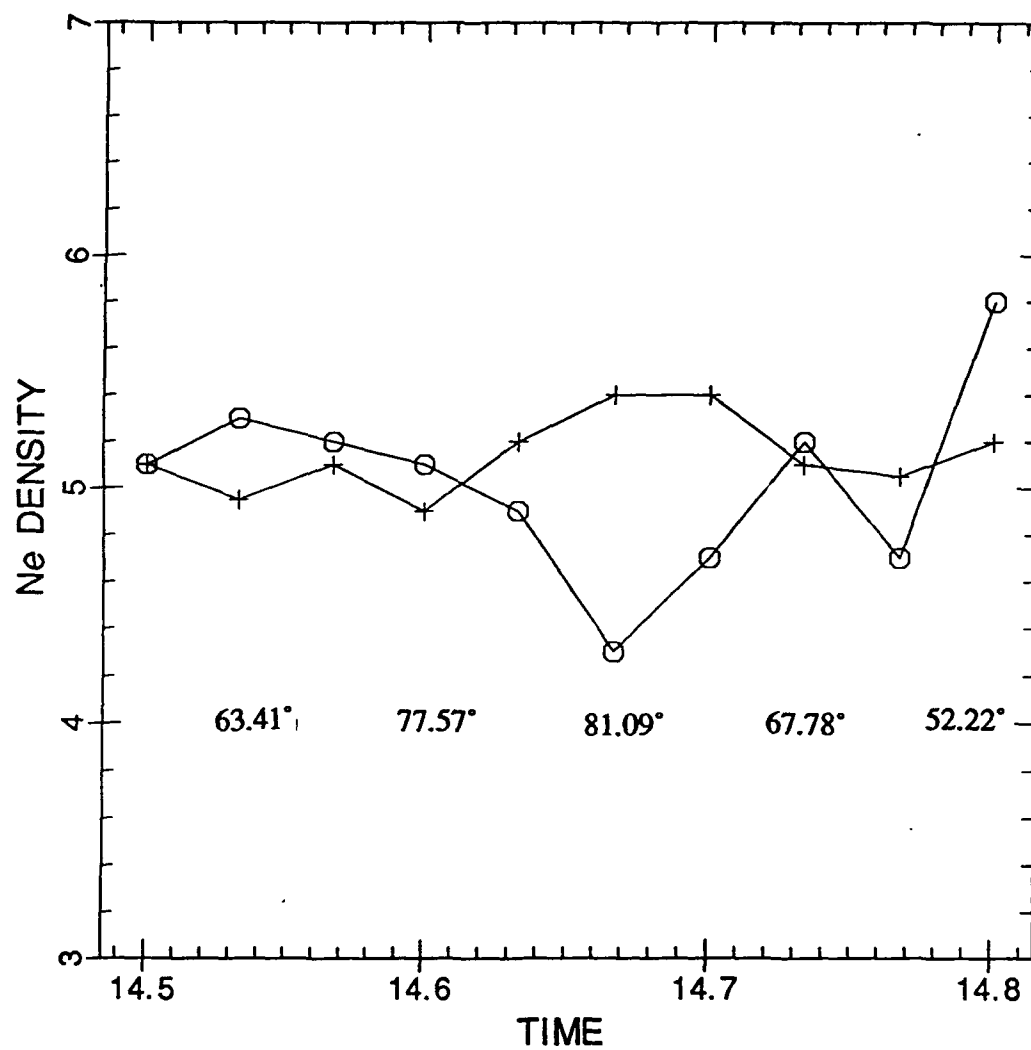


Figure 16. An example of a polar hole in the DE-2 data. Note the density minimum at 81.09°A. It can be seen that the TDIM did not detect the hole at the same location.

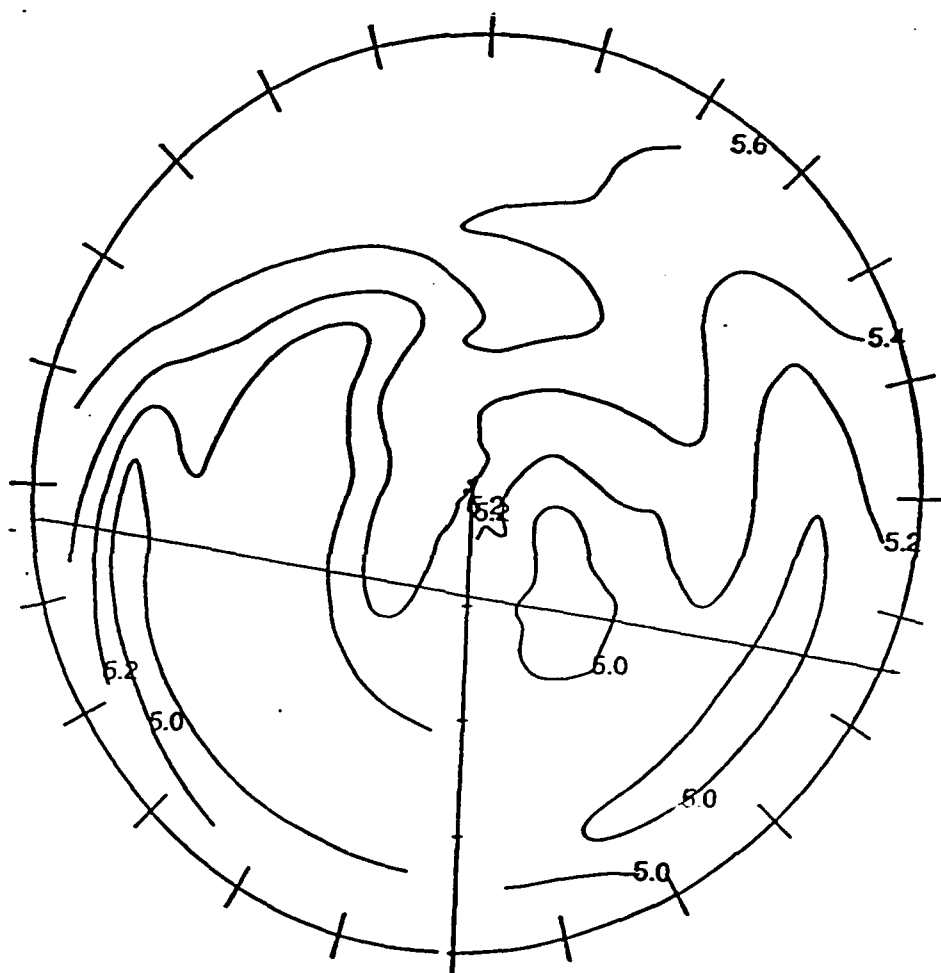


Figure 17. The TDIM plot for the same time frame as Figure 16. Note the appearance of the polar hole on the opposite side of the pole from where the DE-2 data shows it. The superimposed lines are that of the DE-2 orbit.

there were only one or two examples of a polar hole that could be found in the fiche data. The comparison of the TDIM model to the actual observations will be discussed here.

For the most part, the criterion used for placing orbits in this region was a density maximum occurring in the polar region. However, a minimum density was used for polar hole detection. Table 13 shows the results of observations versus model comparison for the polar cap region during both northward and southward IMF conditions. Although the model in this region is better than what was presented in the trough region, there is still room for improvement to possibly aid in making a forecast for this region. Just as in the trough region, if it can be determined where features are located in the polar cap, they could be input into the model to make the model initially accurate. Since most of the features in the polar cap region last for at least a short time, a very short-range forecast could be made from this. Subtle movements of these features could also be detected by subsequent satellite passes and that information could be used to forecast as well. Ultimately, however, as in the trough region, a parameter such as electric field changes will have to be measured to aid more accurately in forecasting polar cap events.

5.3 AURORAL REGION

Another region of the ionosphere is the auroral region. It is generally from about $65^{\circ}\Lambda$ to about $80^{\circ}\Lambda$. However, it is only a few degrees latitude wide at any given time [Jursa, 1985]. Precipitating particles and optical emissions occur throughout the auroral zone. Optical emissions are a result of the energy from precipitating particles (mostly electrons) being deposited in the ionosphere. In the equatorward portion of the aurora, these optical emissions are spatially uniform and are known as diffuse aurora. Along the poleward portion of the oval the precipitating particles tend to be grouped in bands about 1° wide. The precipitating energetic particles lose energy to the atmosphere by ionizing neutrals. In the nighttime F region where ionization lifetimes are long, the ionization present at any

Table 13. Specifications of the polar cap region

	IMF NORTHWARD	IMF SOUTHWARD	TOTAL
Feature evident in model:			
	4/7 (57.1%)	11/16 (68.8%)	15/23 (65.2%)
Feature showed up:			
BEFORE	2/7 (28.6%)	4/16 (25.0%)	6/23 (26.1%)
EXACTLY	0/7 (0.0%)	2/16 (12.5%)	2/23 (8.7%)
AFTER	2/7 (28.6%)	5/16 (31.3%)	7/23 (30.4%)
N/A	3/7 (42.9%)	5/16 (31.3%)	8/23 (34.8%)
Magnitude of feature:			
GREATER	0/7 (0.0%)	2/16 (12.5%)	2/23 (8.7%)
EQUAL TO	0/7 (0.0%)	0/16 (0.0%)	0/23 (0.0%)
LESS THAN	4/7 (57.1%)	9/16 (56.3%)	13/23 (56.5%)
N/A	3/7 (42.9%)	5/16 (31.3%)	8/23 (34.8%)

given moment is influenced by the recent precipitation (tens of minutes) as well as the instantaneous precipitation. It should be pointed out that the DE-2 observations that were looked at were in the F region of the ionosphere. The auroral region has its main activity occurring outside the F region in the E region. So the electron densities and temperatures that were looked at in the auroral region were outside the region of main auroral activity. Vertical and horizontal transport have a major effect upon the structure of the F region. Because of this only the equatorward edge of the auroral region was detectable at this height. If these observations had the capability of looking into the E region, much more activity throughout the entire region might have been observed. In the sunlit aurora zone, photoionization dominates the production of ionization, but ionization from particles has a major effect on plasma irregularities [Jursa, 1985].

All of the above-mentioned factors remain somewhat consistent as long as no changes in the region are taking place. Processes in the auroral region are almost instantaneous so any change to the auroral region will have an almost immediate impact on the processes

taking place in this region. The most important factor that greatly impacts the activity in the auroral region is geomagnetic activity. The biggest geomagnetic changes come during times of substorm activity in the magnetosphere. Here the field lines that connect the magnetosphere to the auroral region of the ionosphere become much more active and cause an immediate increase in precipitation intensity. This may also cause the auroral region to expand equatorward.

So, unlike the trough and polar cap regions where changes occur much slower, this region with its potential for rapid change is tougher to monitor. Here, as in the other regions, a current position of the auroral region may be detected. This can then be put into the model to give an instantaneous representation of the auroral region and the ionosphere. As pointed out above, the change in the auroral zone is much more rapid than that of the trough or polar cap regions. Therefore, it may not be so easy to continuously monitor the exact location of the aurora. One suggestion might be to only try to monitor the equatorward edge of the auroral region. This would give a very short-term forecast on the actual movement of the aurora. Judging by the change in the auroral region that caused this equatorward change (mostly an increase in precipitating particles), a little longer forecast could be made as the aurora continues to expand or tries to return to its quiet conditions. This would still entail monitoring the electric field changes in the auroral region just as needs to be done in the other two regions discussed. Since most of the other two regions have processes that are related to the auroral region, both physical processes and even location (i.e., poleward edge of trough, patches of ionization, etc.) this monitoring of the equatorward and poleward edge of the aurora seems more appropriate than monitoring the actual processes in the region. The electric field changes directly influence the location of both the poleward and equatorward edges of the region so this seems to be the parameter to monitor in conjunction with the movements of the poleward and equatorward edges of the region. It was also noted from the fiche data that there was an electron temperature

increase about 66.7% of the time in the vicinity of the equatorward edge of the auroral region.

In comparing the DE-2 data with the TDIM model a density maximum in the auroral region is assumed to be the equatorward edge of the auroral region. It is sometimes not so obvious where the poleward edge of the aurora lies. The stronger the activity in the auroral region the stronger the *density maximum* and the more defined the equatorward edge is. In this region, as in the trough region, it was possible to detect auroral activity on some orbits both on the ascending part and the descending part of the orbit. Figure 18 shows an example of a plot in the auroral region with good agreement between the model and the observations. The observed density maximum at $77.06^\circ\Lambda$ is assumed to be the equatorward edge of the aurora. Figure 19 shows an example of poor agreement between the model and the observations. Note the presence of an aurora observed on both the ascending and descending orbit and that the TDIM does not really detect either of them. Table 14 shows the comparison of observations versus model comparisons for the auroral region during northward and southward IMF conditions. As in the other regions discussed, an attempt should be made to improve the model in an effort to make a forecast. As before, the measurement of electron temperatures and densities would give current information which could be input into the model, along with current geomagnetic conditions, etc., to give an accurate instantaneous location of the auroral region. But for forecasting purposes, since this region is coupled directly with the magnetosphere, it is these measurements which are most relevant. These include electric field changes, particle precipitation, etc. Due to the quick reaction time in the auroral region, these parameters need to be measured as far "upstream" as possible, because by the time they are detected in the actual ionosphere, it may be too late to forecast anything.

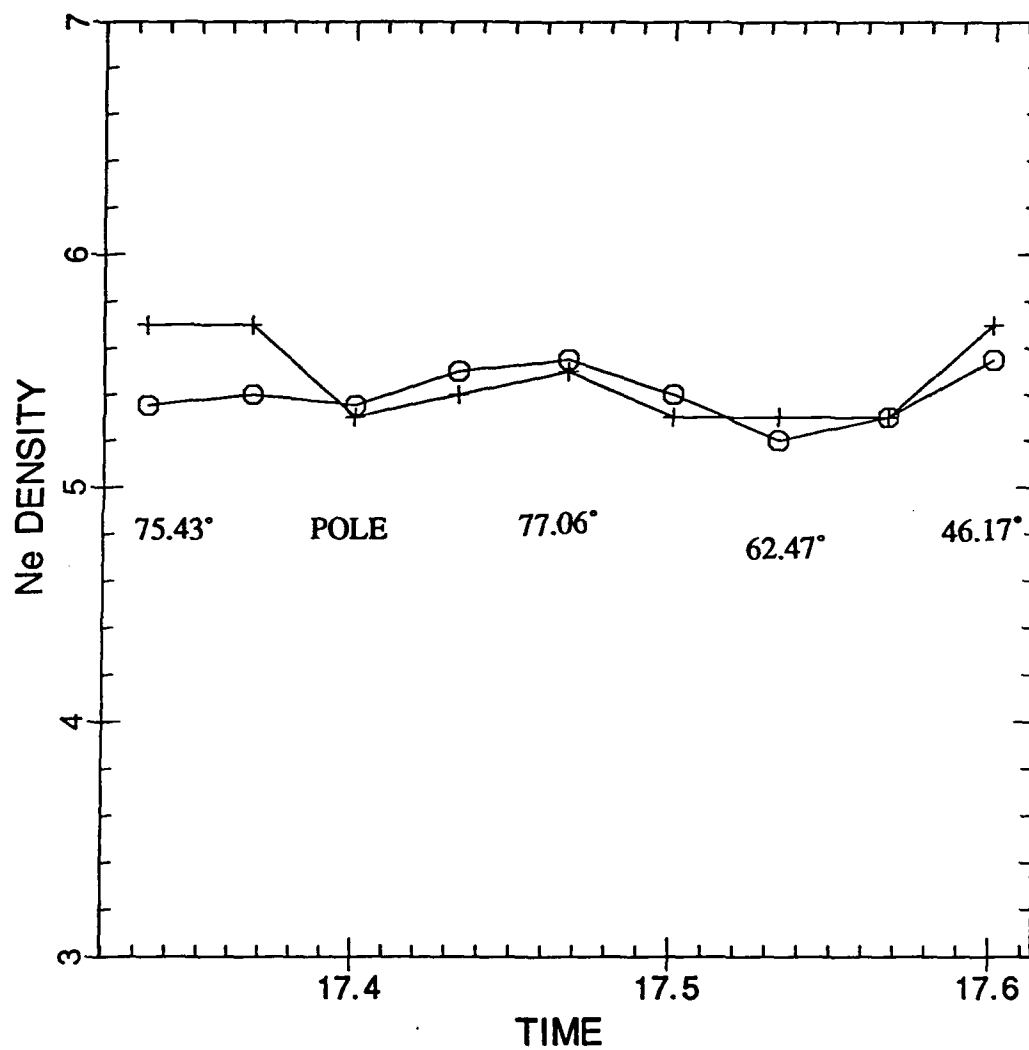


Figure 18. This figure shows good agreement between the observations and the model. The observed edge of the auroral oval is at 77.06°A, which is about the same location as the TDIM places it. Note that the density maximum here is much higher than the polar cap region which implies activity in the auroral region.

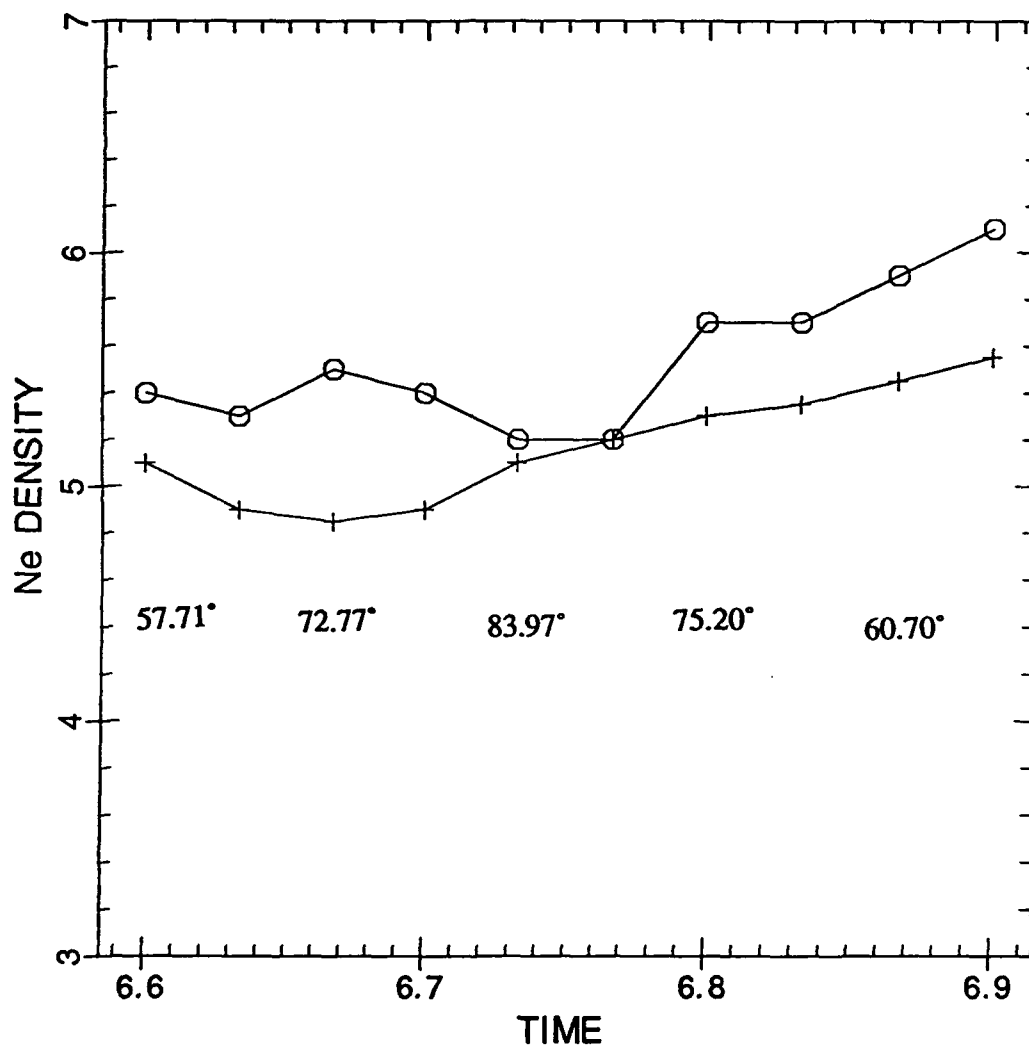


Figure 19. An example of poor agreement between the observations and the model. Note the equatorward edges of the auroral region are noted at $72.77^\circ\Lambda$ ascending and $75.20^\circ\Lambda$ descending. The TDIM does not seem to detect either of these features.

Table 14. Specifications of the auroral region

	IMF NORTHWARD	IMF SOUTHWARD	TOTAL
Feature evident in model:			
	9/15 (60.0%)	3/7 (42.9%)	12/22 (54.5%)
Feature showed up:			
BEFORE	4/15 (26.7%)	1/7 (14.3%)	5/22 (22.7%)
EXACTLY	4/15 (26.7%)	0/7 (0.0%)	4/22 (18.2%)
AFTER	1/15 (6.7%)	2/7 (28.6%)	3/22 (13.6%)
N/A	6/15 (40.0%)	4/7 (57.1%)	10/22 (45.5%)
Magnitude of feature:			
GREATER	0/15 (0.0%)	0/7 (0.0%)	0/22 (0.0%)
EQUAL TO	1/15 (6.7%)	0/7 (0.0%)	1/22 (4.5%)
LESS THAN	8/15 (53.3%)	3/7 (42.9%)	11/22 (50.0%)
N/A	6/15 (40.0%)	4/7 (57.1%)	10/22 (45.5%)

5.4 MID-LATITUDE REGION

The final region of the ionosphere to discuss is the mid-latitude region. This region covers the same latitude range ($50-65^\circ\text{N}$) as the trough region. But instead of density minimums as in the trough region, the concern focuses on density maximums in this region. Tascione [1988] states that the energy deposited into the neutral atmosphere at high latitudes can profoundly influence the mid-latitude ionosphere by changing the atmospheric circulation patterns that determine the neutral gas composition. The maximum electron concentration occurs at the level where downward diffusion and electrons loss by recombination are of equal importance. Other factors which influence processes in the mid-latitude ionosphere include variations in the ratio $\text{O}/(\text{N}_2+\text{O}_2)$, which can lead to variations in peak densities. Vertical ion drift also cause concentrations to shift in this region. Also, exchange of ionization along magnetic field lines between the ionosphere and the plasmasphere is important to maintenance of the nighttime ionosphere. The

equatorward wind, at times, also is a factor in this region, specifically an abatement or reversal of the equatorward wind. There is also a seasonal anomaly in daytime peak densities. Summer densities in the F2 region are usually much higher than winter densities [Tascione, 1988].

The mid-latitude region was the hardest region to place DE-2 orbits into because the density maximums near 65°A could be construed as being the equatorward edge of the auroral region. Electron temperatures were not much help here either because there were just as many orbits with increasing electron temperatures as there were orbits with decreasing electron temperatures over the mid-latitude region.

The processes in the mid-latitude region may also be the result of residuals of the auroral region having penetrated into this region, i.e., as the aurora retreats back to the north after a disturbed period, some increase in densities may be "left behind" for a while longer. Basically, the placing of the orbits in the mid-latitude region was done when a density maximum was visible in the observations but no other explanation existed as to why a maximum should be seen there. Figure 20 shows an example of good agreement between the model and the observation while Figure 21 shows an example of poor agreement between the model and the observations. Table 15 shows the comparison between the observations and the model for the mid-latitude region during northward and southward IMF conditions. While parameters such as electron density and electron temperatures, etc., can be measured in this region, it is not obvious how a forecast can be made for this region without inputs, information etc., from the surrounding regions (auroral, trough). It seems that the changes in this mid-latitude region are directly correlated with changes in other regions and are not independent.

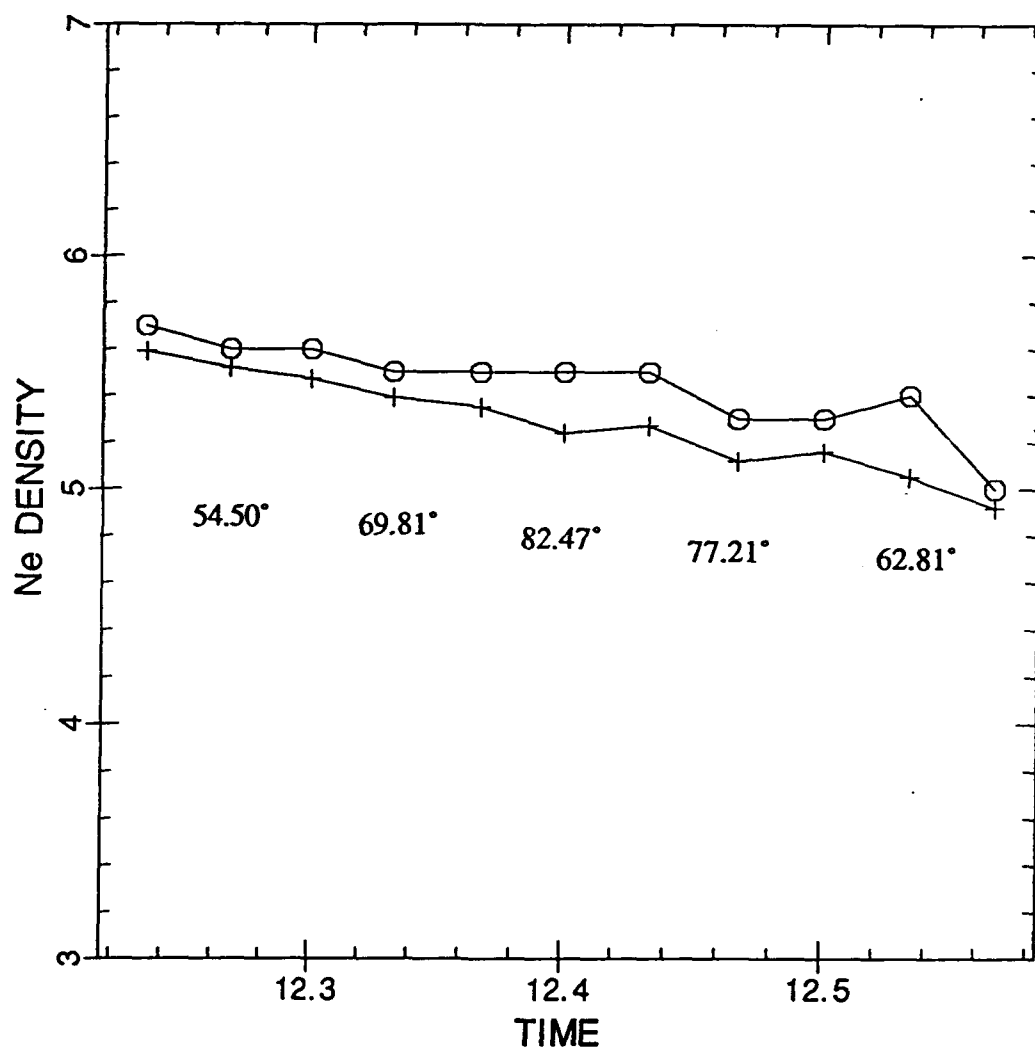


Figure 20. An example of good agreement between the model and the observations. Note that the density maximum is observed at $62.81^{\circ}\Lambda$. While the TDIM does not show a maximum at this particular latitude, it does show one occurring earlier in the orbit ($70.17^{\circ}\Lambda$). The rest of the two curves have excellent similarities.

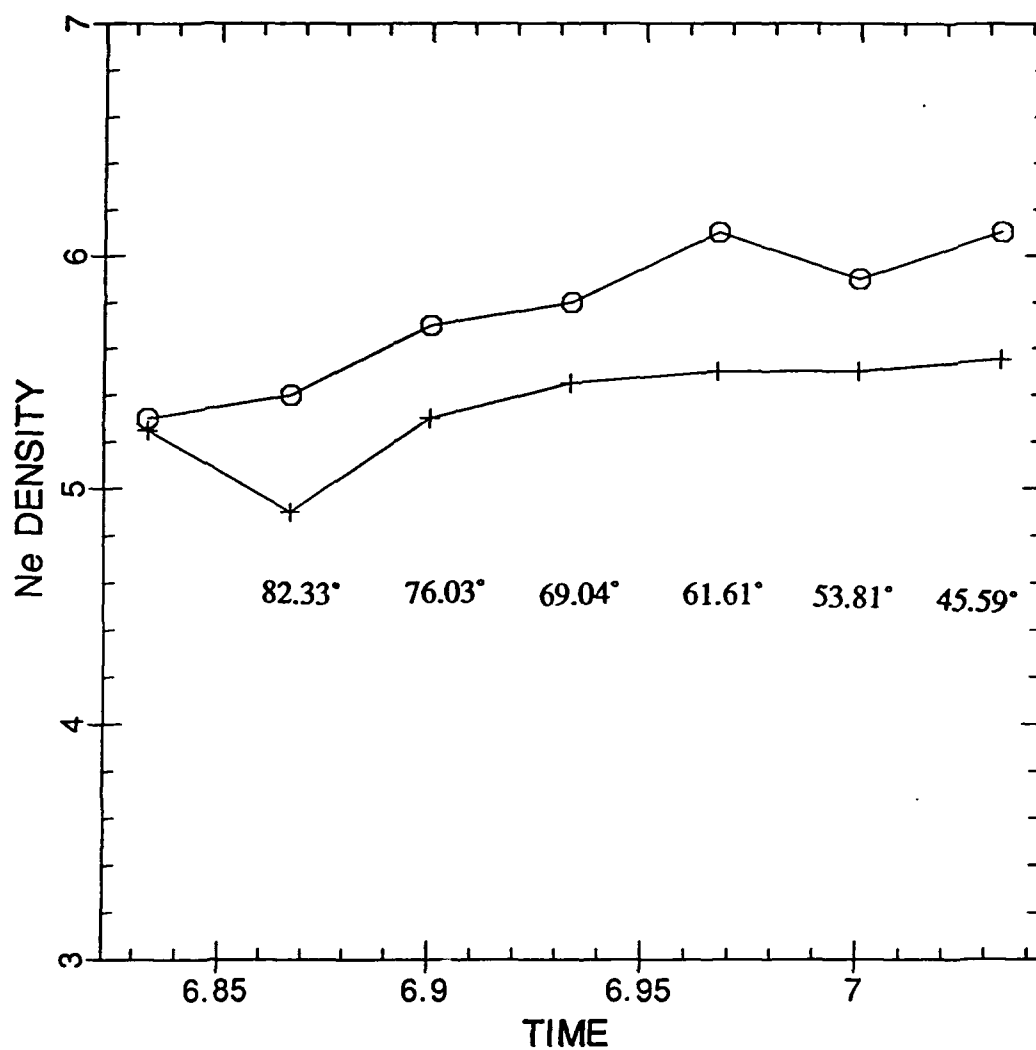


Figure 21. An example of poor agreement between the curves for the mid-latitude region. The density maximum is observed at $61.61^\circ\Lambda$ and the TDIM shows no indication of detecting the feature at all.

Table 15. Specifications of the mid-latitude region

	IMF NORTHWARD	IMF SOUTHWARD	TOTAL
Feature evident in model:			
	5/8 (62.5%)	5/7 (71.4%)	10/15 (66.7%)
Feature showed up:			
BEFORE	1/8 (12.5%)	1/7 (14.3%)	2/15 (13.3%)
EXACTLY	2/8 (25.0%)	3/7 (42.9%)	5/15 (33.3%)
AFTER	2/8 (25.0%)	2/7 (28.6%)	4/15 (26.7%)
N/A	3/8 (37.5%)	1/7 (14.3%)	4/15 (26.7%)
Magnitude of feature:			
GREATER	3/8 (37.5%)	0/7 (0.0%)	3/15 (20.0%)
EQUAL TO	0/8 (0.0%)	0/7 (0.0%)	0/15 (0.0%)
LESS THAN	2/8 (25.0%)	6/7 (85.7%)	8/15 (53.3%)
N/A	3/8 (37.5%)	1/7 (14.3%)	4/15 (26.7%)

5.5 SUMMARY

This chapter has looked at the regions of the ionosphere, their physical characteristics, and how actual data for these regions compared with the models. It has been shown that some parameters in these regions (mostly electron densities and temperatures) can be measured directly to give an instantaneous location to the regions. Other parameters, mainly electric field changes, need to be measured and an appropriate time delay factor needs to be calculated if possible to enable an actual forecast to be made for these regions. In the next chapter an appropriate constellation of observations to measure these parameters will be discussed.

CHAPTER 6

CONCLUSIONS

The objective of this research was to determine an optimum number of observations needed to monitor (measure) the status of the ionosphere to aid in forecasting future ionospheric events. It was first pointed out what kind of job the models are doing in depicting a "present" day ionosphere. The TDIM would depict features but not always in the exact same place or with the exact same magnitude as the observed. But the model is climatological in nature and therefore is showing an "average" over a given time and probably not an instantaneous result as might be acquired from the DE-2 observations. Since these same models will be the ones used to forecast events, there must be an attempt to improve the current depiction of the ionosphere, or in other words, have the model depict the features exactly as they are observed. If this can be done, then an accurate baseline will exist to base a forecast on. The use of satellites may be useful in obtaining more and better data for use in these models.

In selecting orbits for ionospheric analysis in this study, a number of conditions were used, i.e., IMF direction, Kp, season, etc. About 140 orbits were initially selected to be examined. However, only 88 of these orbits actually had pertinent data associated with them on the fiche. The question as to whether this is enough orbits can be addressed by considering the following. From the perspective of model comparison, since the model is climatological only (averages), it is unlikely that more data would change significantly the results of comparing the actual data occurrences to "average" occurrences. Due to the random nature in which the orbits were selected, and the distribution of these orbits, an ample cross section of data would have been looked at and compared with the models. To satisfy that more orbits probably would not have made a difference, other orbits were looked at and their results were recorded but not presented in this work.

Some of the things that were learned as a result of this study are as follows.

1. Moffett and Quegan [1983] state that the poleward edge of a trough is usually steeper than the equatorward edge. This was found to be true only 38.7% of the time from a subjective look at the DE-2 data.

2. While the TDIM does depict features often, it may not always correspond with the features that are actually observed. Therefore, improvement to the TDIM model is a first step to forecasting ionospheric events.

3. From the DE-2 fiche, the presence of the aurora is depicted only by activity in an equatorward boundary and not throughout the entire region as is expected for reasons discussed in Section 5.3.

The main overall result that can be discerned from this thesis is that before a forecast of the ionosphere can be made, an accurate baseline must exist in the models, and currently one does not. This can only be done by using current in situ observations and "pinpointing" the regions where they currently are in the model. These in situ observations can best be taken by satellites orbiting through the region.

Activity that occurs in the ionosphere is very comparable with the weather that is seen here in the troposphere region of the atmosphere. For example, quiet conditions in the ionosphere are like high pressure areas here on Earth. Very little impact to communications systems, satellites, etc., is seen during this time. However, the occurrence of a disturbed period in the ionosphere would affect all the regions, especially with respect to densities, and movements of the particular regions. Regions such as the trough region, if situated over an operationally important area, could interfere dramatically with communication processes. The same effect would be felt in a hurricane here in the troposphere, that is, a disruption of communication, etc. One would need to know present positions and forecast future locations of the ionospheric regions just as one would need to know the present position and forecast future positions of a hurricane so that decisions can be made as to what precautions, if any, to take. So this drives home the point of the importance of

establishing a baseline (present) condition before a forecast is made, as well as continuous monitoring of the region for movement, etc., to update forecasts if necessary. This comparison implies that a more regional concentration is important, i.e., trough region, since the trough does play havoc with the effectiveness of various communications systems here on Earth. Unlike a hurricane, however, the trough region would tend to "rebound" back to its quiet time position, which would imply that unless the location of interest was at the farthest point it would feel the effects of the trough both on the equatorward and poleward progression of the trough. This progression is another example for the need of constant monitoring and an establishment of a baseline condition.

The regions of the ionosphere for the most part are defined by maximum or minimum electron densities, depending on the region. Instrumentation exists which can measure electron densities, electron temperatures, particle composition, etc., which are real-time occurrences and are just the parameters that are needed to help in establishing the location of the ionospheric regions and this information can be input into the model to give an accurate baseline. Unfortunately these parameters, when observed in this real-time mode, are not conducive to forecasting since these are in situ measurements of what is happening now. Parameters such as electric field change, changes in IMF direction, changes in Kp, etc. are some parameters that indicate the changes in the various ionospheric regions. As addressed earlier, it is this cause and effect problem which was looked at in this research. It was determined that there is no one-to-one relationship in cause and effect. It is also impossible to see the driver directly, i.e., energy input is integrated into the F region ionosphere. Also the time constant is from one minute to tens of minutes; hence this is the desired change in time sampling resolution.

If one assumes conjugacy of the ionosphere, then provided one or more of the regions can be located (determined), this region would exist in the same place in both the northern and southern hemisphere and circumscribe the entire world at approximately the same

latitude as the initial observation as described by the model. So, with just one satellite making a polar orbit, a measurement for a particular region could be taken up to four times depending on the season (twice in the northern hemisphere and twice in the southern hemisphere) in about a two-hour period. During the summer season, these regions, especially the trough region, would be seen just once at about midnight local time (LT). The time of one orbit is approximately 110 minutes. This would mean that each region would be passed through once every 27.5 to 30 minutes or so. This time interval might be acceptable if one was just interested in "general" movements of the location of the regions only. A much smaller time interval would be necessary to follow the "progression" of the region, which is more conducive to forecasting. This would be true more for the polar cap region and trough region where formation and decay of the regions require some time. A much smaller time frame is a definite necessity for the auroral region because as stated earlier in this thesis, activity in the auroral region can be explosive, which implies quite a bit of activity could happen in the 30 minutes between passes if only one satellite is used. This particular problem could be overcome by using an auroral imager satellite, which would be used exclusively for monitoring the auroral region movement.

Different orbits would depict different occurrences depending on the orientation of the orbit. For example, assuming a quiet time convection pattern, a noon to midnight orbit would give very little indication as to structure in the ionospheric region. But a dawn to dusk orbit would give a much better indication of areas of ionization, etc. All of this is seasonally dependent as well since, depending on the season, the terminator would be in various positions in the ionosphere, which would cause varying effects depending on the season.

Polar orbiting satellites seem to be the way to go since this method would provide global coverage. Geostationary satellites would tend to monitor just a certain area and may miss out on key or significant features that are occurring elsewhere. While three to six

geostationary satellites would probably be enough to view the ionosphere generally, due to the obliqueness of the orbits, some regions of the ionosphere would be looked at very little.

Methods of accomplishing the optimal observations of the ionosphere are as follows.

One consideration is that parameters can be measured by observations from ground-based stations. In fact, ground stations currently exist that give ionospheric data. Since ground-based stations are capable of taking constant measurements in one place, if a feature is passing over one of these stations, it would probably be detected. So, it may be feasible to put the satellites in an orbit that do not pass over the ground stations, since this might imply a duplication of data. It may be better to have the satellites offset from the ground-based stations to add credibility to a feature occurring in a specific area. Going back to the conjugacy assumption again, if the ground-based station detects a feature, then the satellite should detect it as well. The converse of this is not necessarily true however. That is if the satellite detects a feature, the ground-based station may not. This is because the satellite would be moving through the area of the feature whereas for ground-based stations, the feature would be moving over the station. A feature could be occurring in a region and never be detected by ground-based stations. No configuration of ground-based stations would be able to give total coverage of the ionosphere but the observations from any ground-based station could be used to update the model and to possibly improve the baseline ionospheric depiction needed for a successful forecast. Advantages and disadvantages of ground-based stations alone are listed in Table 16. The number of satellites needed would depend on the desired resolution needed to forecast. Since the polar cap and the trough region are relatively slow to change, a time interval of five to 10 minutes between "passes" is probably adequate. F region topside time constants are from one minute to tens of minutes. While this probably would not detect any immediate change in the auroral region, it probably would be quick enough to detect the change soon after it

Table 16. Advantages and disadvantages of ground-based stations alone

ADVANTAGES

- Continuous monitoring of parameters in the ionosphere in one location.
- Current arrangement allows for monitoring along the same longitude (only in certain political regions). The east coast of the United States is a good example.
- Easier maintenance of equipment at the station.
- Easier (direct) access to data from the station.

DISADVANTAGES

- If significant occurrence in the ionosphere was happening away from the station, it would not be seen.
 - Various ionospheric regions might not be detected nor the movement of these regions detected either.
 - Under current arrangement activity happening at other longitudes would not be seen.
 - Data would be relevant for only a few hours (LT) a day.
 - Fixed local time is more important than co-rotating at one longitude (i.e., 1800 always means electric field across polar cap etc.)
-

happened and then an adjustment can be made to the forecast if needed. The auroral imager mentioned earlier could help here.

One might argue that an even smaller time resolution is desirable. While this may be true, it does not seem like much would be gained in the final forecast because of the relatively slow change of the polar cap and trough regions. Also, other regions would not be observed with this same high resolution. Hence improving dramatically one region but not everywhere would not be a net gain. While this smaller time resolution would be favorable for possible auroral region activity, it should be remembered that satellites orbit a certain distance above the ionosphere so that the parameters that cause auroral activity (mostly from the magnetosphere and the solar wind) could be intercepted (and therefore

detected) by an orbiting satellite before the parameters even reach the ionospheric auroral region and thus give a "heads up" that a change is probably imminent by responding to sudden changes. This would basically involve monitoring the IMF and looking for a sudden change in the direction of the IMF since this would probably change the current status of the ionosphere. A drastic change in Kp, particularly from a relatively low value to a relatively high value, would be important also. Kp is only currently reported in three hourly values however. So a smaller Kp increment would be required. Work would be needed to produce five-minute Kp models. At the present time these do not exist.

Another consideration is that only one satellite would be needed at any given latitude to detect a region because of our previous assumption of conjugacy. Therefore, any series of satellites in a polar orbit (running along any longitude line) would detect any region if it was detectable. So all that would be needed would be a series of satellites orbiting around one "longitude" instead of many satellites circling many longitudes.

So, the number of satellites required to monitor the ionosphere assuming a 10-minute time interval and a "longitudinal" arrangement of the satellites would be 11 (110 minutes ÷ 10 minute interval = 11 satellites). This 10-minute resolution gives potential across polar cap, auroral fluxes, auroral bands, trough location, and heating in a "key" MLT sector, which would constrain model inputs and identify baseline ionosphere. Here the TDIM would have time history for inputs and also be validated in real time. This would be about the minimum required to give enough data to the models to make a decent forecast. Figure 22 shows one idealized orbit that may work during equinox conditions since about the same amount of daylight and darkness is present during this time. Any singular orbit no matter what its orientation (probably LT dependent) would miss certain parameters at certain times of the year. Table 17 shows some parameters that should be measured on this time interval and their significance in the ionosphere. Obviously, even more satellites would give more data about the regions to input to the models. This would result in

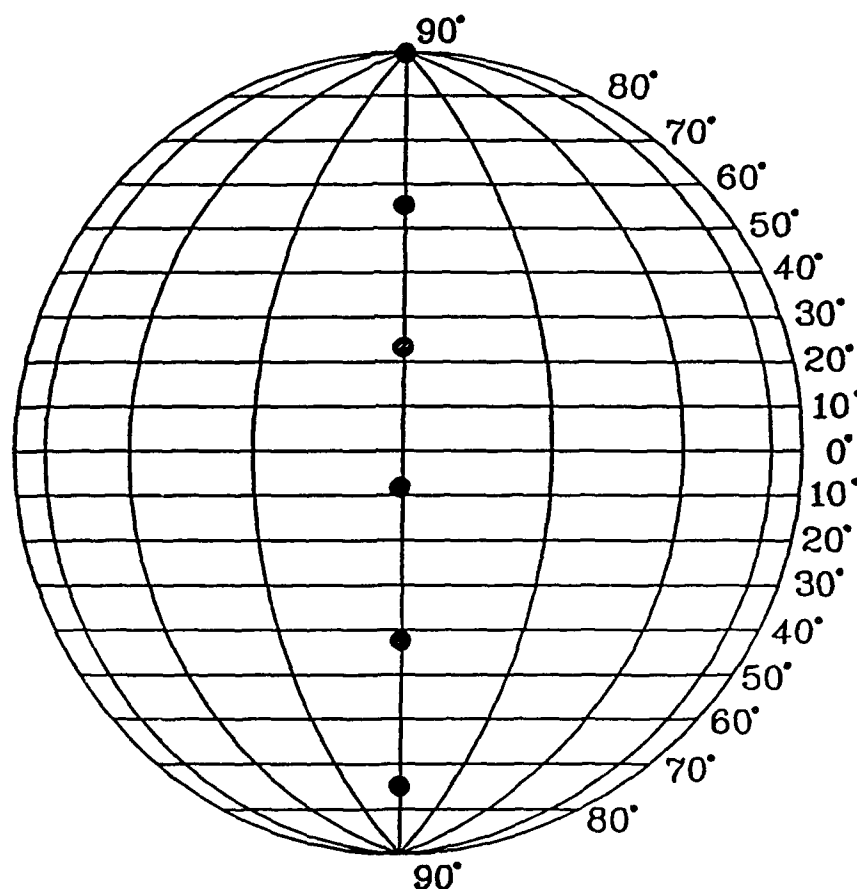


Figure 22. This figure shows approximate spacing required for satellite constellation to give a 10 minute interval between points. There should be about 33° latitude between each satellite. This "polar orbit" alignment of the satellites seems to be the best orientation to observe changes in all of the mid and high latitude ionospheric regions with a minimal number of satellites. Additional longitude lines are not necessarily drawn to scale and are drawn for illustrative purposes only. This figure shows only one side of the orbit. This implies that satellites are also on the other side of the orbit as well with approximately the same spacing as shown here, but they are not necessarily "directly across" from the satellites on this side of the orbit.

Table 17. Parameters that should be measured on a smaller time scale

<u>PARAMETER</u>	<u>REASONING</u>
Electron Density	An increase or decrease in density would assist in locating various ionospheric regions. Monitoring on a 5-minute time scale could show the progression (movement) of the various regions.
Electron temperatures	While temperatures alone cannot help in locating regions in the ionosphere, a change in temperatures along with a change in density can help to identify the regions. As with density, a 5 minute time scale can help to show movement of the various regions. Also, an increase in temperature could imply a deepening trough, etc.
Electric field	This measurement on a 5-minute or so time scale could give "immediate" input to a forecast. To a degree, both density and temperature are affected by electric field changes so any change observed now would result in a change of one or both of the above a short time later. Also the continuous monitoring means that realistic time history of $E(x,y,z)$ is available.
Particle composition	This when accompanied with other parameters can show movement of regions because certain ions are only present in certain regions which would then help classify a region. Also the continuous monitoring means that realistic time history of $E(x,y,z)$ is available.
IMF	A change in the IMF from one direction to another would cause significant changes to occur in the ionosphere.
Instantaneous Kp	Somewhat related to the previous one in that the intensity of the Kp may tell to what extent the ionosphere would be changing. This would be much quicker than the present Kp currently being used.

instantaneous changes (dependent on the exact time interval) so that a more accurate rate of change can be observed and by extrapolation maybe a more accurate forecast could be made. Table 18 addresses the advantages and disadvantages of these satellites in just one orbit.

The question to be considered now is what sort of orbit (shape, height, etc.) would give the best ionospheric coverage? Obviously one requirement is that the satellite has to pass over every latitude sometime during the orbit. Also, as alluded to previously, an orbit that passes high enough above the ionosphere to pass through as many field lines from the magnetosphere as possible is desirable. But since the satellites should remain close to the ionosphere itself, a circular or nearly circular orbit would give maximum coverage as well as maximize the lifetime of the satellite. Table 19 shows a summary of this one orbit scenario.

Due to the possible changing of the orbit or variations in orbits of different local times (LT) and the seasonal variation as well (as discussed previously), more than one orbit would probably be required since there would be certain times of the year when no relevant data to aid in placement of the regions would be obtained. Expanding this one orbit concept to two or more different orbits would allow for more of the ionosphere to be monitored and also would permit monitoring during times when just the single orbit would not be able to measure parameters. It also would enable more spatial structure in $E(x,y,z)$ inputs, precipitation, troughs, polar holes, polar tongues, etc. Advantages and disadvantages of this two or more orbit scenario are in Table 20. Figure 23 depicts two orbits, which could be used to monitor the ionosphere with better coverage than one orbit. Note that while this specific example does not exactly give a dawn-to-dusk orbit or a noon-to-midnight orbit, it does cover the premidnight and predawn regions as well as the morning and afternoon sectors. Table 21 shows a summary of this two-orbit scenario.

Maximum monitoring of the ionosphere could be done sufficiently with about two

Table 18. Advantages and disadvantages of satellites (one orbit only) *

ADVANTAGES

- Monitoring of the entire ionosphere is possible to note location and movement of the regions.
- "Instantaneous" changes in the ionosphere can be detected.
- Monitoring of parameters that are incoming to the ionosphere from the magnetosphere and the solar wind are possible.

DISADVANTAGES

- Seasonal aspects of the ionosphere would make it so during certain times of the year, satellites would not be collecting data that would be relevant to region monitoring.
- Maintaining equipment is not so easy. If equipment or satellite dies, then a data void exists.
- Potential problem with data acquisition on the ground.

* Orbit would be in a longitudinal or "local time" orbit.

Table 19. One orbit plane configuration (Scenario 1)

Number of satellites : 11

$\Delta t = 10$ minutes

Local time: 1800 - 0600 LT

Altitude: 600 - 800 km.

Measurements: electric fields
 particle precipitation
 n_e, n_i, t_e, t_i , composition

Table 20. Advantages and disadvantages of 2 or more different orbits *

ADVANTAGES

- This arrangement would allow for global monitoring of ionosphere throughout the year.
- It would be easier to locate and "follow" regions in the ionosphere.
- Could measure the ionosphere closer to the noon-midnight and dawn-dusk orbits.
- An increased chance in monitoring IMF changes and changes from magnetosphere and/or solar wind into the ionospheric region exists.
- Instantaneous monitoring of changes in the ionosphere.
- There is a decrease in the chances of data void areas happening.

DISADVANTAGES

- Maintenance of equipment (satellites) is not easy.
 - Potential problem exists with immediate data acquisition on the ground.
-

* Orbits would be different longitudinal or "local time" orbits.

separate orbits of satellites and an augmentation/complementation by ground-based stations to help in establishing the baseline required in the model before a forecast can be made. Table 22 shows the advantages and disadvantages of these combined efforts.

Further research should establish how the intensity of changes of the drivers of the ionosphere cause the other parameters to change, i.e., what changes occur when a little change in drivers is seen as opposed to a big change in drivers, etc. This would be useful when a baseline is established in the models.

Also, a better understanding of the drivers before they enter the ionosphere, i.e., electric currents, energy, etc., in the magnetosphere and magnetosphere-solar wind coupling, could give even more lead time to a forecast in the ionosphere.

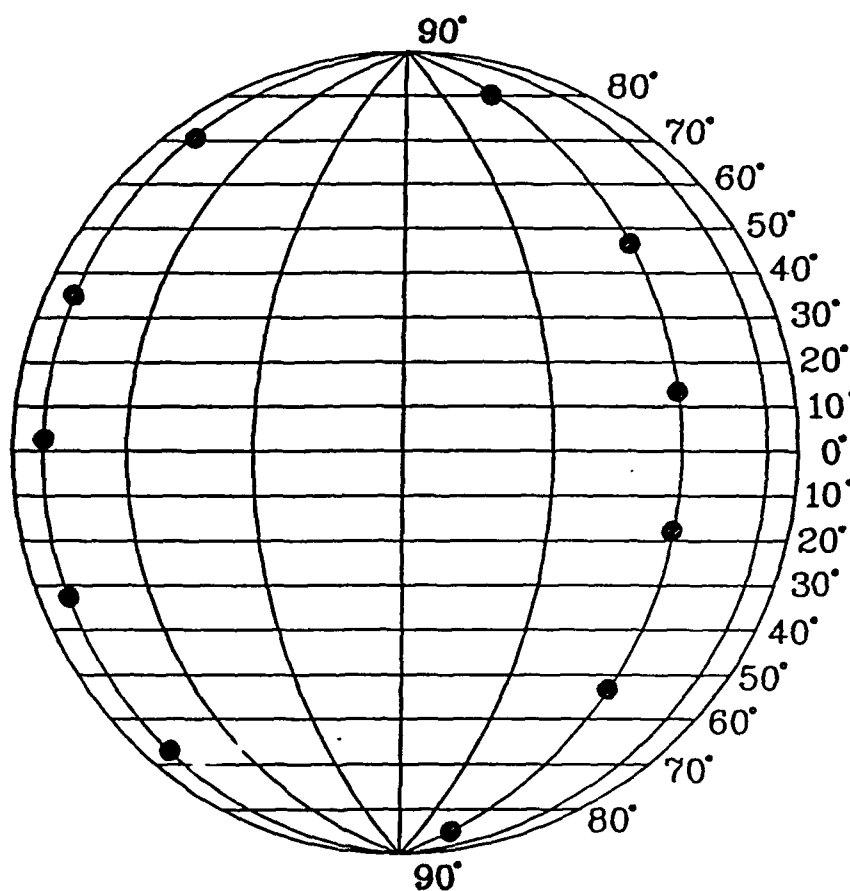


Figure 23. One of many possibilities for coverage of the ionosphere using more than one orbit (2 in this case). Using a configuration of more than one orbit allows for more ionospheric coverage. It also ensures that all of the ionosphere is covered (and therefore all the parameters are observed) throughout the entire year. It is not limited as one orbit is by seasonal and diurnal effects. Multiple orbits are possible but it would seem that more than 3 or 4 orbits would cause unnecessary duplication of detection of features as well as increase the chance for some catastrophe to take place in space, i.e., a collision between satellites or other spacecraft, etc. It should be remembered that this figure shows only half of an orbit. The other half would be "into the page."

Table 21. Two orbit plane configuration (Scenario 2)

Number of satellites : 22, (11 for each orbit)

$\Delta t = 10$ minutes

Local time orbit 1: 2000 - 0800 LT

Local time orbit 2: 1600 - 0400 LT

Altitude: 600 - 800 km.

Measurements: electric fields
particle precipitation
 n_e, n_i, t_e, t_i , composition
location of polar holes, tongues of ionization, etc.

Table 22. Advantages and disadvantages of both ground-based stations and satellites

ADVANTAGES

- (All of the above mentioned advantages plus)
- Combination of data to input to models to improve baseline would exist.
- Ground station could make data acquisition easier. If orbits of satellites were such that the ground based station could receive data from the satellite as well then data from both the ground and satellite could be transmitted to users on the ground simultaneously.
- The present ground based configuration could be considered as "part of 1 orbit" so satellites could be in another orbit different from the ground based one.

DISADVANTAGES

- (All of the previously mentioned disadvantages plus)
- A potential for data overlap (duplication at times) exists. This would not be the most beneficial use of resources.

So the bottom line is that while measurements of the ionosphere can be made by satellites, some sort of improvement needs to be made to the models before any sort of ionospheric forecasting can be successfully accomplished. Once this is established, then more measurements from the satellites can be used to create or improve a forecast.

REFERENCES

- Anderson, D.N., J. Buchau, and R.A. Heelis, Origin of density enhancements in the winter polar cap ionosphere, *Radio Sci.*, 23, 513-519, 1988.
- Baumjohann, W., Merits and Limitations of the Use of Geomagnetic Indices in Solar Wind-Magnetosphere Coupling Studies, *Solar Wind-Magnetosphere Coupling*, Terra Scientific Publishing Co., 3-15, 1986.
- Brown, L.D., R.E. Daniell, Jr., M.W. Fox, J.A. Klobuchar, and P.H. Doherty, Evaluation of six ionospheric models as predictors of total electron content, *Radio Sci.*, 26, 1007-1015, 1991.
- Buchau, J., E.J. Weber, D.N. Anderson, H.C. Carlson, Jr., J.G. Moore, B.W. Reinisch, and R.C. Livingston, Ionospheric structures in the polar cap: Their origin and relation to 250-MHz scintillation, *Radio Sci.*, 20, 325-338, 1985.
- Caudal, G., and M. Blanc, Magnetospheric convection during quiet or moderately disturbed times, *Rev. Geophys.*, 26(4), 809-822, 1988.
- Frank, L.A., J.D. Craven, D.A. Gurnett, S.D. Shawhan, D.R. Weimer, J.L. Burch, J.D. Winningham, C.R. Chappell, J.H. Waite, R.A. Heelis, N.C. Maynard, M. Sugiura, W.K. Peterson, and E.G. Shelley, The theta aurora, *J. Geophys. Res.*, 91, 3177-3224, 1986.
- Gussenhoven, M.S., Low-altitude convection, precipitation, and current patterns in the baseline magnetosphere, *Rev. Geophys.*, 26(4), 792-808, 1988.
- Hoffman, R.A., G.D. Hogan, and R.C. Maehl, Dynamics Explorer spacecraft and ground operations systems, *Space Sci. Instrum.*, 5, 349-367, 1981.
- Jursa, A.S., *Handbook of Geophysics and Space Environment*, Air Force Geophysics Laboratory, 1985.
- Köhnlein, W., and W.J. Raitt, Position of the mid-latitude trough in the topside ionosphere as deduced from ESRO 4 observations, *Planet. Space Sci.*, 25, 600-602, 1977.
- Moffett, R.J., and S. Quegan, The mid-latitude trough in the electron concentration of the ionospheric F-layer: a review of observations and modeling, *J. Atmos. Terr. Phys.*, 45, 315-343, 1983.
- Niciejewski, R.J., J.W. Meriwether, Jr., F.G. McCormac, J.H. Hecht, A.B. Christensen, G.G. Sivjee, D.J. Strickland, G. Swenson, S.B. Mende, A. Vallance Jones, R.L. Gattinger, H.C. Carlson, and C.E. Valladares, Coordinated satellite and ground-based measurements of the energy characteristics of a sun-aligned arc over Sonde Stromfjord, *J. Geophys. Res.*, 94, 17201-17213, 1989.
- Schunk, R.W., A mathematical model of the middle and high latitude ionosphere, *Pure Appl. Geophys.*, 127, 255-303, 1988.

- Sojka, J.J., Global scale, physical models of the F region ionosphere, *Rev. Geophys.*, 27, 371-403, 1989.
- Sojka, J.J., R.W. Schunk, W.R. Hoegy, and J.M. Grebowsky, Model and observation comparison of the universal time and IMF By dependence of the ionospheric polar hole, *Adv.Space Res.*, 11, (10)39 - (10)42, 1991.
- Stern, D.P., Energetics of the magnetosphere, *Space Sci. Rev.*, 39, 193-213, 1984.
- Tasicone, T.F., *Introduction to the Space Environment*, Orbit Book Co., 82-85, 1988.
- Valladares, C.E., and H.C. Carlson, Jr., The electrodynamic, thermal, and energetic character of intense sun-aligned arcs in the polar cap, *J. Geophys. Res.*, 96, 1379-1400, 1991.

APPENDIX

Table 23. Northward IMF breakdown into regions

REGION	SEASON	NUMBER OF OCCURRENCES		PERCENTAGE OF TOTAL - SEASON
		HI K _p	LO K _p	
TROUGH	SPRING	2	2	44.4
	SUMMER	1	1	25.0
	AUTUMN	1	2	25.0
	WINTER	0	2	16.7
MID-LAT	SPRING	1	1	22.2
	SUMMER	1	0	12.5
	AUTUMN	1	0	8.3
	WINTER	1	1	16.7
AURORA	SPRING	2	1	33.3
	SUMMER	0	1	12.5
	AUTUMN	1	1	16.7
	WINTER	1	3	33.3
POLAR CAP	SPRING	0	0	0.0
	SUMMER	2	0	25.0
	AUTUMN	0	3	25.0
	WINTER	2	0	16.7
NOT WELL DEFINED	SPRING	0	0	0.0
	SUMMER	0	2	25.0
	AUTUMN	2	1	25.0
	WINTER	0	2	16.7

TOTAL ORBITS = 41

AVERAGE BY REGION:	TROUGH	26.8%
	MID-LAT	14.6%
	AURORAL	24.4%
	POLAR CAP	17.1%
	NOT WELL DEFINED	17.1%

Table 24. Southward IMF breakdown into regions

REGION	SEASON	NUMBER OF OCCURRENCES		PERCENTAGE OF TOTAL - SEASON
		HI Kp	LO Kp	
TROUGH	SPRING	1	0	8.3
	SUMMER	3	0	33.3
	AUTUMN	2	2	30.8
	WINTER	0	1	7.7
MID-LAT	SPRING	1	1	16.7
	SUMMER	0	1	11.1
	AUTUMN	1	2	23.3
	WINTER	1	0	7.7
AURORA	SPRING	1	1	16.7
	SUMMER	1	0	11.1
	AUTUMN	0	1	7.7
	WINTER	0	1	7.7
POLAR CAP	SPRING	2	3	41.7
	SUMMER	1	1	22.2
	AUTUMN	3	0	23.1
	WINTER	2	4	46.2
NOT WELL DEFINED	SPRING	1	1	16.7
	SUMMER	0	2	22.2
	AUTUMN	1	1	15.4
	WINTER	2	2	30.8

TOTAL ORBITS = 47

AVERAGE BY REGION: TROUGH	19.1%
MID-LAT	14.9%
AURORAL	10.6%
POLAR CAP	34.0%
NOT WELL DEFINED	21.3%

Table 25. Curve comparisons for trough conditions

OBSERVED MODEL						
DAY	TDIM	IRI	LENGTH	LENGTH	MAGNITUDE	OCCURS
NORTHWARD IMF						
82076	F	P	< 2 min	< 2 min	less	before
82101	G	P	< 2 min	< 2 min	same	before
82078	F	P	< 2 min	< 2 min	less	before
82088	F	P	< 2 min	< 2 min	less	exact
82146	F	P	< 2 min	≈ 6 min	less	exact
82169	P	P	< 2 min	< 2 min	less	after
82268	P	P	< 2 min	< 4 min	less	after
			< 2 min	< 2 min	NA	NA
82278	F	P	< 2 min	< 2 min	greater	exact
82263	P	P	< 2 min	NA	NA	NA
82335	F	P	< 2 min	< 2 min	less	exact
			< 2 min	< 2 min	less	exact
82336	F	P	≈ 6 min	≈ 6 min	same	exact
			< 2 min	≈ 4 min	less	exact
SOUTHWARD IMF						
82094	F	P	< 2 min	NA	NA	NA
82164	F	P	< 2 min	< 2 min	less	exact
82165	G	P	≈ 6 min	NA	NA	NA
82214	P	P	< 2 min	NA	NA	NA
			< 2 min	NA	NA	NA
81295	F	P	< 2 min	< 2 min	same	exact
82280	F	P	< 2 min	≈ 4 min	greater	exact
81237	G	P	< 2 min	< 2 min	less	exact
82279	P	P	< 2 min	NA	NA	NA
81328	P	P	< 2 min	NA	NA	NA
			< 2 min	NA	NA	NA

Table 26. Curve comparisons for mid-latitude conditions

			OBSERVED MODEL			
DAY	TDIM	IRI	LENGTH	LENGTH	MAGNITUDE	OCCURS
NORTHWARD IMF						
82060	F	P	< 2 min	< 2 min	greater	after
82068	P	P	< 2 min	NA	NA	NA
82195	P	P	≈ 6 min	< 2 min	greater	exact
			≈ 4 min	NA	NA	NA
82264	F	P	< 2 min	< 2 min	less	exact
82344	F	P	< 2 min	< 2 min	less	after
			< 2 min	≈ 4 min	greater	before
81357	F	P	< 2 min	NA	NA	NA
SOUTHWARD IMF						
82080	P	P	< 2 min	< 2 min	less	after
82038	F	P	2 min	2 min	less	exact
82183	F	P	< 2 min	< 2 min	less	before
82269	P	P	< 2 min	NA	NA	NA
81239	P	P	≈ 4 min	≈ 4 min	less	after
81259	P	P	≈ 4 min	≈ 4 min	less	exact
81346	F	P	≈ 4 min	< 2 min	less	exact

Table 27. Curve comparisons for auroral oval conditions

			OBSERVED MODEL			
DAY	TDIM	IRI	LENGTH	LENGTH	MAGNITUDE	OCCURS
NORTHWARD IMF						
82042	P	P	< 2 min	≈ 4 min	same	exact
82091	P	P	< 2 min	< 2 min	less	before
82083	P	P	< 2 min	NA	NA	NA
			< 2 min	NA	NA	NA
82204	F	P	< 2 min	≈ 4 min	less	before
81239	G	P	< 2 min	< 2 min	less	exact
82257	F	P	< 2 min	< 2 min	less	before
			< 2 min	< 2 min	less	before
82354	F	P	< 2 min	≈ 4 min	less	exact
			< 2 min	NA	NA	NA
81356	F	P	< 4 min	NA	NA	NA
			< 4 min	NA	NA	NA
81357	F	P	< 2 min	NA	NA	NA
			< 2 min	< 2 min	less	exact
82002	P	P	< 2 min	< 2 min	less	after
SOUTHWARD IMF						
82053	P	P	< 2 min	NA	NA	NA
			< 2 min	NA	NA	NA
82097	F	P	< 4 min	< 4 min	less	after
			< 2 min	< 2 min	less	after
82193	F	P	< 2 min	NA	NA	NA
81247	G	P	< 2 min	< 2 min	less	before
81337	P	P	< 2 min	NA	NA	NA

Table 28. Curve comparisons for polar cap conditions

OBSERVED MODEL						
DAY	TDIM	IRI	LENGTH	LENGTH	MAGNITUDE	OCCURS
NORTHWARD IMF						
82157	F	P	< 2 min	< 2 min	less	after
82205	F	P	< 2 min	< 2 min	less	before
81236	F	P	< 2 min	NA	NA	NA
81238	P	P	≈ 6 min	NA	NA	NA
81251	F	P	≈ 4 min	< 2 min	less	exact
82030	P	P	< 2 min	NA	NA	NA
82033	F	P	< 2 min	< 2 min	less	before
SOUTHWARD IMF						
82061	F	P	< 2 min	≈ 6 min	greater	after
82100	P	P	< 2 min	NA	NA	NA
82054	F	P	≈ 6 min	NA	NA	NA
82067	P	P	≈ 4 min	NA	NA	NA
82125	F	P	< 2 min	< 2 min	less	after
82205	G	P	< 2 min	< 2 min	less	after
82167	G	F	< 2 min	< 2 min	less	exact
81284	F	P	< 2 min	NA	NA	NA
81293	P	P	≈ 4 min	NA	NA	NA
82302	F	P	≈ 4 min	< 2 min	less	after
82035	F	P	< 2 min	< 2 min	less	after
82342	F	P	< 2 min	≈ 4 min	greater	exact
81311	F	P	≈ 6 min	≈ 8 min	less	before
81324	F	P	≈ 4 min	≈ 2 min	less	before
81340	G	P	< 2 min	≈ 6 min	less	before
81341	F	F	< 2 min	< 2 min	less	before